2016

Development of an enzymatic glucose biosensor for applications in wearable sweat-based sensing

Allison Anne Cargill
Iowa State University

Development of an enzymatic glucose biosensor for applications in wearable sweat-based sensing

by

Allison A. Cargill

A thesis submitted to the graduate faculty

in partial fulfillment of the requirements for the degree of

MASTER OF SCIENCE

Major: Mechanical Engineering

Program of Study Committee:
Jonathan C. Claussen, Major Professor
Ellen McKinney
Eliot Winer

Iowa State University

Ames, Iowa

2016

TABLE OF CONTENTS

LIST OF FIGURES

LIST OF TABLES

NOMENCLATURE

BSA	Bovine Serum Albumin
CNT	Carbon Nanotube
DMF	N,N-Dimethylformamide
GOx	Glucose Oxidase from *Aspergillus Niger*
Pt-CNT	Platinum-Decorated Carbon Nanotube
SDS	Sodium N-Dodecyl Sulfate

ACKNOWLEDGMENTS

I would like to thank my major professor, Dr. Jonathan C. Claussen, and my committee members, Dr. Eliot Winer and Dr. Ellen McKinney, for their guidance and support throughout the course of this research. I am grateful for the opportunity to contribute to such exciting research, and thank Dr. Claussen for encouraging, teaching, and supporting me throughout my time in graduate school.

In addition, I would like to extend my sincere thanks to the students and staff in the Claussen Lab Group for their encouragement, support, and assistance with experiments. In particular – Suprem Das, John Hondred, Qing He, Shaowei Ding, Bolin Chen, Kshama Parate, Nate Garland, and Loreen Stromberg – it has been a privilege to work with you! To the undergraduate and high school students that I worked with, thank you for your patience and willingness to help on all types of tasks.

Finally, I would like to thank my family and friends, especially my parents, Greg and Pat, and my brother, Jeff, who supported my decision to attend graduate school and provided constant encouragement.

ABSTRACT

The recent development and commercial availability of wearable devices like the FITBIT® and Apple Watch® reflect an increasing consumer interest in actively monitoring health parameters. Though wearable devices are beginning to emerge in a variety of fields and applications, there is particular interest in the development of wearable monitors for continuously sensing blood glucose levels. Diabetes currently affects nearly 10% of the American population, a number that is expected to rise in the near future, prompting increased interest in noninvasive methods of monitoring glucose levels. This interest in noninvasive monitoring and the recent advent of continuous monitoring products like the FITBIT® are coupled together in the concept of wearable glucose sensors that utilize sweat glucose concentration levels as a means to monitor blood glucose concentration.

This work centers on sweat-based glucose biosensors with applications in continuous monitoring for diabetes patients. It includes an overview of glucose biosensors and an introduction to electrochemistry (Chapter 1) and an investigation into the effectiveness of electrodeposited platinum nanoparticles as a transduction element in electrochemical glucose biosensor (Chapter 2).

A large part of this thesis (Chapter 3) is devoted to the development of an entirely inkjet printable working electrode for applications in wearable sensing. The developed electrode was fabricated entirely through inkjet printing using a commercially available Fujifilm Dimatix Materials Printer and characterization tests show that the sensor performs similarly to sensors fabricated using more costly and time-intensive clean room methods. The sensor consists of a conductive graphene underlayer, an insulative lacquer

coating which serves to maintain constant electrode surface area, a transduction layer of platinum-decorated carbon nanotubes, a detection layer of glucose oxidase and stabilizing protein bovine serum albumin, and finally, a cross-linking layer of glutaraldehyde. When operating in phosphate buffer solution the sensor demonstrates a linear sensing range of 10 µM to 2.51 mM glucose, which is within the range of sweat glucose concentrations, a response time of 18 seconds, average sensitivity of 18.09 µA mM^{-1} cm^{-2}, and a theoretical detection limit of 3.79 µM glucose.

CHAPTER 1: INTRODUCTION

Biosensors

Biosensors – analytical devices that are based on recognition of a biological element[1] – have experienced phenomenal growth since the first biosensor was introduced by Leland C. Clark, Jr., and Champ Lyons in 1962. Biosensors have extremely broad applications and can be found in a variety of industries ranging from healthcare to agriculture to defense. The global market for biosensors is quite large and only expected to grow in coming years as interest in food quality, health care monitoring, disease diagnostics, and national security continue to develop.

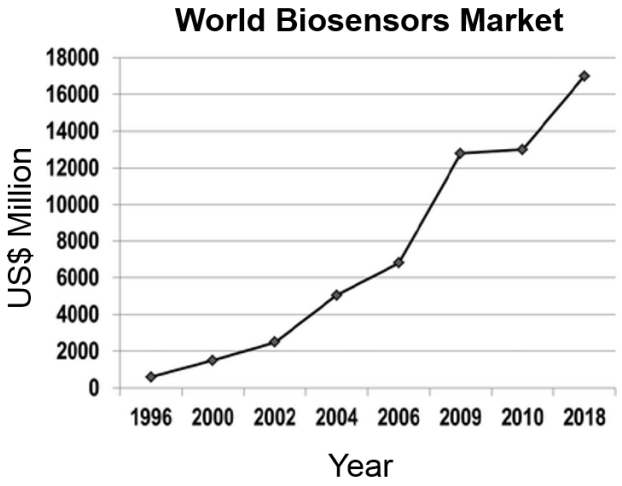

Figure 1. Graph of the world market for biosensors estimated from various commercial sources and predicted for the future in US$ millions. Reproduced from Turner 2013[1] with permission from The Royal Society of Chemistry.

The term "biosensor" accurately implies sensing using a biological component, and all biosensors utilize this concept in some capacity. However, there are many different types of biosensors – different purposes, different components, and different characteristics – all of which make biosensing a very diverse, complex field. In order to understand relevant literature some terminology must be defined. The biosensor system

has its foundation in three key elements: recognition (sensing), signal transduction, and detection (Figure 2).[2] The recognition element in a biosensor is the selective component that allows the biosensor to monitor one particular event, often protein binding, and is absolutely critical in order for the biosensor to have any chance of functioning. The transduction element is the component (often physical) that transduces, or converts, the biological signal generated from the recognition element into a usable signal, usually an electrical signal. Finally, the detection element monitors the signal output from the transduction element. After information has passed the detection element of a biosensor the transduced signal is often output on a display for the end user to process, and the biosensor has completed its work. It is important to note that even in biosensors with the same end function (e.g., monitoring pH), these three elements may be designed very differently. Most biosensors can be broken down into separate elements that fit into the classifications presented in Figure 2, although there are a variety of ways this can be accomplished. This diversity in biosensor operating methods and functional components make this field extremely diverse, and the constantly-changing landscape of technical capabilities ensures that growth in the field of biosensors will never be stagnant.

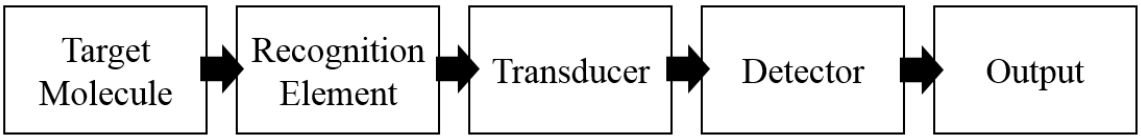

Figure 2. Functionality of a biosensor broken down into steps. First the target molecule interacts with the sensor's recognition element, often via a biological binding event. The transducer then converts the biological signal into a usable (often electrical) signal and sends it to the detector. The signal is monitored by the detector, and the final reading is displayed on an output.

Glucose sensors

Diabetes mellitus is a relatively common disease affecting nearly 10% of the American population.[3] This disease affects the body's ability to process the energy in food, and managing it often requires monitoring blood sugar (glucose) levels throughout the day.[4,5] In fact, careful monitoring and control of blood sugar have been shown to reduce side effects often associated with diabetes including amputation and organ failure.[1] The numbers of adults with diabetes is expected to increase 55% by the year 2035,[6] so it should come as no surprise that glucose biosensors comprise approximately 85% of the global biosensor market.[7]

By far the most common method of testing blood sugar is by using blood glucose test strips that are read by a glucometer. This method of testing is considered invasive, as it requires a fresh sample of blood from the patient, but results are extremely accurate and the meters are easy to use, often presenting a reading in a matter of seconds.[8] The test strips contain glucose oxidase, an enzyme that selectively binds to glucose. Once the patient collects a fresh blood sample and inserts it into the meter, an electrochemical reaction is monitored to determine the concentration of glucose in the sample.[9] This monitoring method is not only invasive, causing pain and potential nerve damage, but it must be done 3-4 times throughout the day, requiring patients to alter their schedules and physically keep supplies with them. Alternatively, a continuous monitoring system would alleviate these problems. To the user's benefit, studies have shown that continuous monitoring can lead to a more accurate picture of prolonged blood glucose trends, which would help in treatment of the disease.[5,10]

Continuous monitoring systems

Continuous monitoring systems are considered by many to be the future of glucose monitoring.[1,11] Within the scope of continuous monitoring devices, there are an abundance of different methodologies that have been demonstrated as feasible means of monitoring real-time glucose levels. The most delineating feature between them is the biological fluid they use as a sensing medium. Continuous glucose monitors have been demonstrated using human blood, serum, sweat, tear fluid, interstitial fluid, and saliva as the sensing medium with certain advantages and disadvantages to each (Table 1). Sweat was selected as the sensing medium for this project as it is easily accessible, its volume can be increased by inducing certain environmental conditions such as high temperature or humidity, and a sweat-based glucose sensor has great potential to be incorporated into a wearable device.

It is important to note that research studies are not in agreement on the range of glucose concentration found in human sweat; rather, the amount of glucose found in human sweat varies significantly. Figure 3 presents a comparison of different studies on the concentration of glucose in human sweat. The average lower limit seen in the literature is approximately 10 μm.[12-14] This measurement was selected as the target lower limit of detection for the context of this thesis. In order to make sweat-based sensing a reality, additional medical research studies should be performed to determine the actual range of glucose concentration found in human sweat.

There has also been some controversy surrounding how closely sweat glucose levels correlate to blood glucose levels.[13] One recent study discovered high correlation between the two values,[13] but more work should be done to reinforce this finding. In

addition, though the relationship in concentration is highly linear, the degree to which sweat concentration is lower than blood glucose concentration differs between individuals.[12,14,15] To compensate for this, continuous sweat-based glucose monitors would need to be specifically calibrated for individual users to ensure that sweat glucose measurements are accurate.

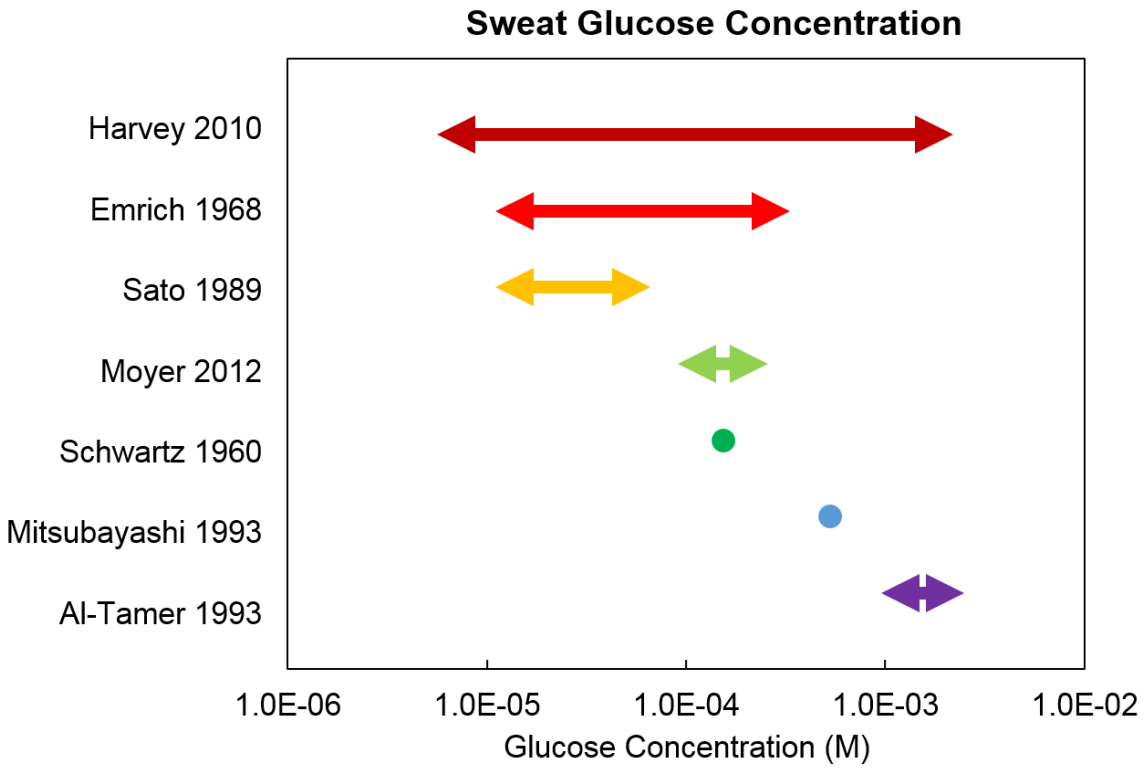

Figure 3. A comparison between the ranges in human sweat glucose concentration found in the literature. Note that the x-axis (glucose concentration) is logarithmic; the literature does not agree on one single range.

Electrochemical biosensors

Biosensors function using a wide variety of sensing approaches: electrochemistry, impedance spectroscopy, colorimetric assays, micro-mechanical systems (e.g., cantilevers), and magnetic fields, to name a few. The most common method utilized by

Table 1. Biological medium used in sensing blood glucose concentration levels and their commonly associated advantages and disadvantages.

Medium	Advantages	Disadvantages
Whole blood	• Most accurate reading	• Most invasive [7]
Serum	• Higher reading than whole-blood [7]	• Processing required • Invasive (serum is derived from whole blood)
Sweat	• Completely noninvasive collection • Mean lag time behind blood glucose concentration: 8 minutes [13] • Glucose concentration is independent of sweat rate [16]	• Sweat rate is activity and environment-dependent • Can be easily contaminated by compounds on the skin • May be up to 100-fold lower than blood glucose concentration [13]
Interstitial fluid	• Mean lag time behind blood glucose concentration: 6.7 minutes [7,17] • ISF levels fall faster than blood glucose levels (hypoglycaemia indicator) [18]	• Lag time can be extensive (patient-dependent) [7] • Need to be calibrated to blood glucose levels at regular intervals [19] • Sample may not be representative of entire body / overall levels [7]
Tear fluid	• Linear correlation to blood glucose concentration [20] • Accessible with common contact lenses [21,22]	• Concentration is 10-fold lower than blood glucose concentration [23] • Interfering proteins present [21] • Large pH shifts day to night [24]
Saliva	• Semi-invasive collection	• May be up to 100-fold lower than blood glucose concentration [25] • Many interfering substances present [19] • Variable lag time [25]
Urine	• Noninvasive collection	• Individual differences in excretion threshold of glucose concentration [25] • Would not allow for continuous monitoring

glucose biosensors is electrochemistry.[2] This section is intended to be a brief overview of electrochemical principles so that the content of this paper can be fully understood.

Electrochemistry refers to the conversion of chemical energy into electrical energy and vice versa.[26] The projects within this thesis all utilize a three electrode set up (Figure 4). In this system, three electrodes – a working, reference, and counter – are placed in an electrolytic conducting solution and individually connected to a potentiostat, a piece of electrical equipment that controls voltage potentials. An electrical current passes between the working and counter electrodes, while a voltage potential is monitored between the working and reference electrodes. From this base configuration many different programs can be run to monitor different system parameters, the most common being cyclic voltammetry (current is monitored as voltage is varied) and chronoamperometry (current is monitored over time, voltage is set at a fixed potential).

The working electrode is where the reaction itself takes place. This is almost always where the biological component is located, and is usually the novel focus in most biosensors. Within most biosensors the counter electrode and reference electrode are standards that are easily purchased from suppliers. The most common type of reference electrode is a liquid Ag/AgCl electrode, which consists of a silver wire coated with silver chloride submerged in a sodium chloride solution.[27] The counter electrode is often simply a platinum wire, and its function is to provide a physical surface to counter the redox reaction occurring at the working electrode.

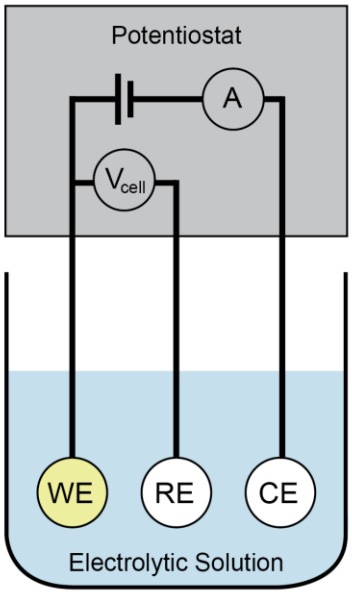

Figure 4. A three electrode setup is commonly used in electrochemical biosensing. In this configuration, the working electrode (WE), reference electrode (RE), and counter electrode (RE) are submerged in an electrolytic (conducting) solution and connected to a potentiostat. Current passes between the WE and CE and voltage between the WE and RE is monitored. This work focuses on the WE, highlighted in yellow.

Biosensor characterization

Biosensor performance is dependent on many different parameters and often evaluated using a variety of methods and metrics. Several parameters that are commonly reported include response time, sensitivity, and stability,[28] but depending on the application and working environment of the sensor, others can also be reported. Glucose sensors, particularly commonplace blood glucose test strips, must be selective, rapid, and reliable,[19] requirements that translate to sensitivity, response time, and stability, respectively. In addition to these three characteristics, linear sensing range and detection limit are two additional characteristics that should be reported for a complete picture of sensor performance.[29] These parameters are relatively easy to determine for amperometric glucose biosensors. Response time can be calculated directly from the raw

data obtained using chronoamperometry. Once this data set has been processed to depend on analyte concentration instead of time, the linear range, sensitivity, and detection limit can all be calculated. Stability, also referred to as shelf life, can be reported in many ways, but is commonly described as the percentage of original signal response after a given amount of time. Figure 5 summarizes these performance indicators and explains how each metric can be calculated.

It is important to consider biosensor performance both in a holistic sense and in the context of the sensor's anticipated applications. For example, a biosensor used in cancer diagnostics may have an acceptable response time that is orders of magnitude greater than the required response time for a blood glucose biosensor. The working fluid (biological sample) requirement for each biosensor also affects the importance of certain metrics, particularly the selectivity of the biosensor. A biosensor that is operating in a complex medium such as human perspiration or a soil sample will need to be able to selectively sense the target analyte and ignore other substances present in the sample, whereas a sample used in laboratory diagnostics could be filtered to eliminate interfering substances. In the context of sweat-based sensing, an effective biosensor must react only to changes in concentration of the target analyte and not show any response to changes in other analytes found in the sweat.

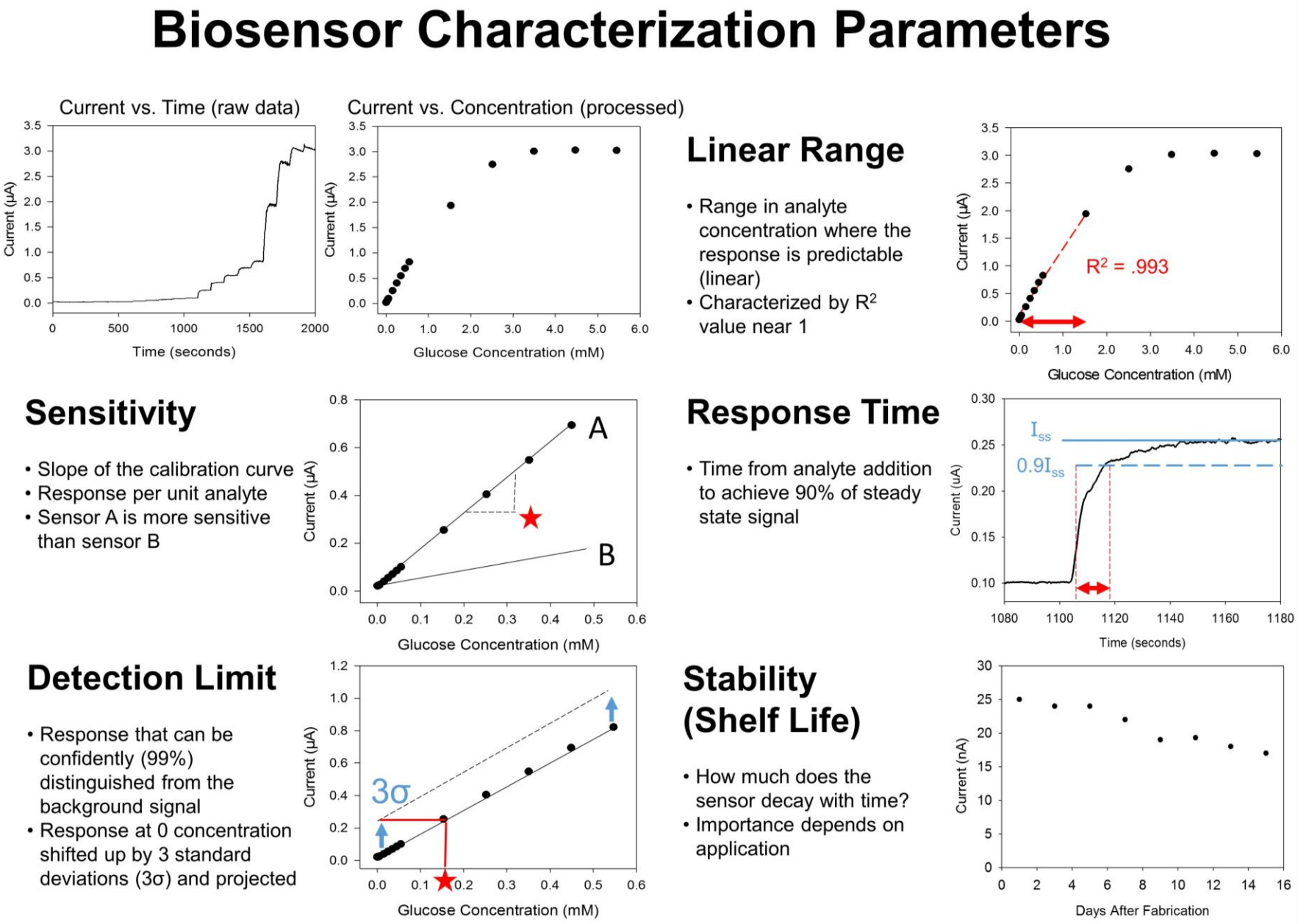

Figure 5. The five parameters that are commonly used to describe electrochemical amperometric biosensor performance. The response time is calculated from the raw current-time data, while the sensitivity, detection limit, and linear range are calculated from the processed current-concentration plot.

CHAPTER 2

EFFECT OF PLATINUM NANOPARTICLE DEPOSITION PARAMETERS ON HYDROGEN PEROXIDE TRANSDUCTION FOR APPLICATIONS IN WEARABLE ELECTROCHEMICAL GLUCOSE BIOSENSORS

Allison A. Cargill,[1] Kathrine M. Neil,[1] John A. Hondred,[1] Eric. S. McLamore,[2] Jonathan C. Claussen[1*]

[1]Department of Mechanical Engineering, Iowa State University, USA
[2]Department of Agricultural and Biological Engineering, University of Florida, USA

Published in Proc. SPIE 9863, Smart Biomedical and Physiological Sensor Technology XIII, 98630E (May 13, 2016)

Reprinted with permission from SPIE. doi:10.1117/12.2227204.

Abstract

Enhanced interest in wearable biosensor technology over the past decade is directly related to the increasing prevalence of diabetes and the associated requirement of daily blood glucose monitoring. In this work we investigate the platinum-carbon transduction element used in traditional first-generation glucose biosensors which rely on the concentration of hydrogen peroxide produced by the glucose–glucose oxidase binding scheme. We electrodeposit platinum nanoparticles on a commercially-available screen printed carbon electrode by stepping an applied current between 0 and 7.12 mA/cm^2 for a varying number of cycles. Next, we examine the trends in deposition and the effect that the number of deposition cycles has on the sensitivity of electrochemical glucose sensing. Results from this work indicate that applying platinum nanoparticles to screen printed carbon via electrodeposition from a metal salt solution improves overall biosensor sensitivity. This work also pinpoints the amount of platinum (i.e., number of deposition

cycles) that maximizes biosensor sensitivity in an effort to minimize the use of the precious metals, viz., platinum, in electrode fabrication. In summary, this work quantifies the relationship between platinum electrodeposition and sensor performance, which is crucial in designing and producing cost-effective sensors.

Introduction

The field of biosensing has rapidly expanded in the past decade from an evaluation of $5 billion in 2004[7] to a projected total market value of $22.7 billion by 2020.[30] While this extreme growth can be attributed to the prevalence of diabetes in developed nations,[7] the term 'biosensor' has expanded beyond traditional blood glucose sensors used for diabetes management to include wearable fitness monitors and activity trackers, cancer diagnostic mechanisms, and even gene identification tools. As of 2013 *wearable* biosensors held a market share of 80% of the total biosensor market,[30] thus making the development of wearable sensors an attractive research focus.

While wearable sensors of many types are of interest, there is a specific need for the development of a noninvasive, wearable glucose monitoring system. Traditional blood glucose sensors are invasive, requiring users to draw blood for glucose measurements, which can be painful, time consuming, and poses the potential to transmit blood borne disease.[31] A recent thrust in the field has been the development of noninvasive sensors that utilize biological media other than blood – such as sweat,[32] tears,[33] or interstitial fluid[34] – as a sensing medium. In particular, sweat-based sensing is an attractive alternative because of its readily available and easily accessible

(noninvasive) supply and diverse composition in that it contains many biomarkers of interest.

This work contributes to the overarching goal of developing a wearable biosensor capable of monitoring real-time glucose levels in human sweat. While several sweat-based glucose monitors have been published[22,32,35] they are proof-of-concept studies and do not contain a thorough analysis or optimization of the glucose sensors within the context of sweat-based sensing. Here we seek to deepen knowledge of the effect of platinum electrodeposition on glucose sensor sensitivity.

Though a variety of detection mechanisms exist for the glucose–glucose oxidase system, one of the simplest consists of measuring the generation of hydrogen peroxide[36] in a method classified as first-generation glucose biosensing. In short, at an applied voltage bias, glucose oxidase catalyzes the conversion of glucose to gluconolactone, producing hydrogen peroxide as a byproduct. Then, platinum catalyzes the reduction of hydrogen peroxide, an electroactive species, of which electrons are a byproduct (Figure 6).[37] Thus, platinum is a common component in first-generation glucose biosensors that measure the concentration of liberated hydrogen peroxide.[38] Furthermore, the use of platinum on the nanoscale in either the nanoparticle or nanowire morphology has been reported to further increase the sensitivity of first-generation glucose biosensors due to the high catalytic efficiency of said nanoparticles.[39,40]

While platinum nanoparticles have been shown to enhance the electrochemical response of glucose–glucose oxidase glucose sensors due to their electrocatalytic behavior towards hydrogen peroxide,[41-44] few reports have tackled the challenge of directly comparing the effects of the density and morphology of platinum nanostructures

and their effectiveness of hydrogen peroxide catalysis with regards to glucose biosensing. We have previously published on the optimal current density for the electrodeposition of platinum onto graphene petal nanosheets[45] and on networks of single-walled carbon nanotubes (SWCNTs)[46-48] and microelectrodes as well as other precious metals such as gold and palladium electrodeposited within porous anodic alumina pores for the creation of nanoelectrode arrays[49] and on networks of SWCNTs[50] for enzymatic-based, electrochemical biosensing.[45] Furthermore we have explored electroless platinum nanoparticle/nanowire deposition techniques for the decomposition of hydrogen peroxide on both carbon nanotube[51] and paper-based substrates.[52] In this work, we build upon these previous research reports by further exploring the relationship between biosensor sensitivity and platinum deposition and seek to determine the minimum amount of platinum nanoparticle surface coverage required to maximize the sensitivity of first generation glucose biosensors developed on screen printed electrodes.

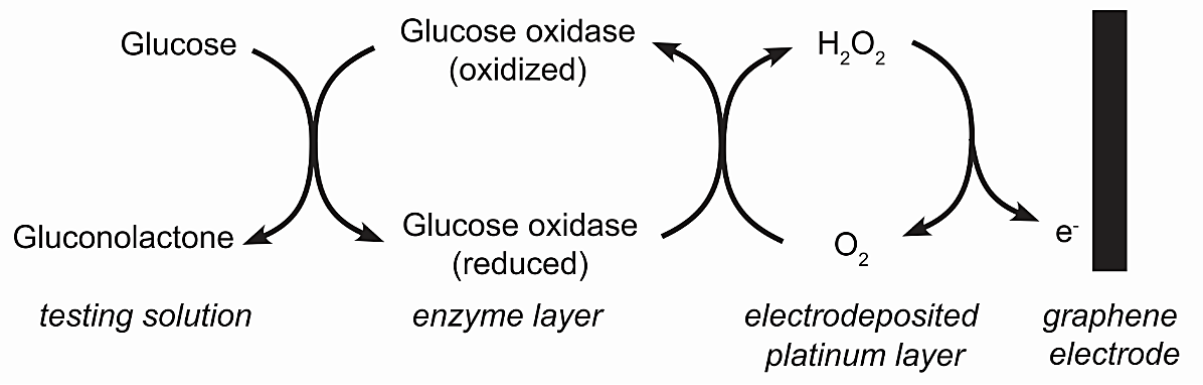

Figure 6. The enzymatic reduction and oxidation scheme that is used in first-generation glucose biosensors and the respective layer where each process occurs for the sensors demonstrated in this work. The process should be viewed from left to right and begins with the addition of glucose to the testing system and culminates when electrons are transferred to the carbon electrode, which is detectable as an increase in current.

Methodology

Preparation of electrodes

Platinum nanoparticles were deposited on the surface of the working electrode following our previous current-pulse, 3-electrode electrodeposition protocols for platinum deposition on graphene nanopetals and carbon nanopetals.[45,46,50,53] The working electrode was a screen printed carbon electrode (CH Instruments SE101), the reference was liquid Ag/AgCl (CH Instruments, CHI 111), and the counter was a platinum wire (CH Instruments, CHI 115). All three electrodes were submerged in electroplating solution [$H_2PtCl_6 \cdot 6H_2O$ (4 mM) and Na_2SO_4 (0.5 M)], and the same solution was used for each deposition. As evidenced in our previous work, the optimal current density for the deposition of platinum on a carbon-based electrode, viz., graphene nanopetals, for glucose sensing applications was 7.14 mA/cm^2.[45] Therefore, current pulses (500 ms) of 7.14 mA/cm^2 were utilized in varying cycles to fabricate each sample.

Glucose oxidase immobilization

Glucose oxidase membranes were fabricated by first mixing equal volumes of glucose oxidase from *aspergillus niger* (Type X-S, Sigma Aldrich G7141) dissolved in PBS (1x, Sigma Aldrich) at a concentration of 8 mg/mL with bovine serum albumin (lyophilized powder, Sigma Aldrich A2153) dissolved in deionized water at a concentration of 80 mg/mL. Then 2.5% glutaraldehyde in water (created from Sigma Aldrich G7776) was added to the compound, mixed via pipette mixing, and a volume of 5 µL was immediately drop coated onto the platinized electrodes. The functionalized electrodes were allowed to dry for 12 hours at room temperature and were rinsed with deionized water prior to testing.

Electrochemical measurements

All electrochemical measurements were conducted using a CH Instruments potentiostat (600E series) operating at an applied potential of +0.4 V. A common three electrode setup was used with the glucose oxidase-functionalized carbon electrode acting as the working electrode, platinum wire (CH Instruments, CHI 115) for the counter electrode, and liquid 3M Ag/AgCl (CH Instruments, CHI 111) for the reference. All tests were conducted in 10 mL PBS (1x, Sigma Aldrich) with a stir bar rotating at 725 rpm. Glucose stock solutions of concentrations 1 mM, 10 mM, 100 mM and 1 M were prepared by dissolving glucose (D-(+)-Glucose, Sigma Aldrich G8270) in PBS and were allowed to sit at room temperature for at least 24 hours prior to testing. Sensors were tested in sets of three to ensure accuracy.

SEM imaging

The electrodeposited platinum was investigated using a Field Emission Scanning Electron Microscope (FE-SEM) [FEI Quanta 250]. Images were captured in atomic backscattered electron (ABS) mode operating at 10 kV with a working distance of approximately 10 mm.

Results and discussion

Platinum is a well-known transduction element used in glucose biosensing, and electrodeposition of platinum nanoparticles is an established technique.[54] By depositing platinum nanoparticles via electrodeposition, a transduction layer that is highly sensitive to hydrogen peroxide can be created on top of a conductive substrate (in this case, carbon). Then, a membrane containing the recognition element, glucose oxidase, can be

applied via drop coating application, effectively creating a complete sensor (see Figure 7). The optimal current density under which to deposit platinum for effective electrochemical sensing has been published as 7.14 mA/cm^2 for a study in which current density was varied while the number of cycles of application remained constant.[45]

In order to begin this study an electrode was prepared with 100 cycles of platinum electrodeposited at a current density of 7.14 mA/cm^2. The complete amperometric response to glucose oxidase over three orders of magnitude is shown in Figure 8 with the linear calibration shown in the inset. The results indicate a large linear sensing range of 1 µM to 2 mM, which closely matches the known range of glucose in sweat.[12,14] In addition, the sensor demonstrated a low theoretical detection limit (calculated to be .718 µM) and fast response time of 21 seconds (defined as the length of time from the glucose injection to a current reading corresponding to 90% of the steady state value).

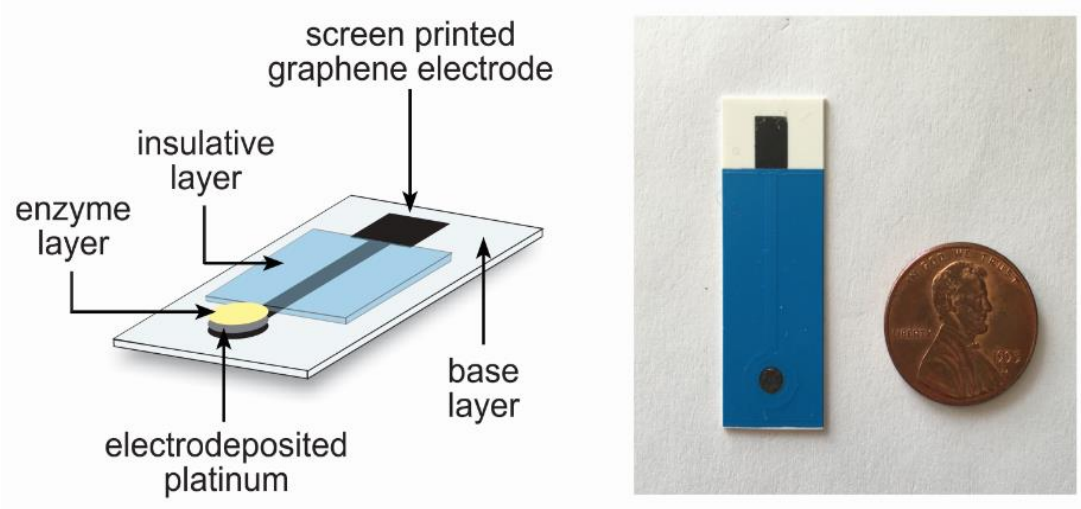

Figure 7. The diagram on the left shows the multilayered, functionalized sensor that is used for testing. The yellow color of the enzyme solution has been exaggerated for identification. The photograph on the right depicts a tested sensor next to a penny.

Subsequently, additional sensors were fabricated with platinum being deposited in an increasing number of cycles. SEM images of the electrodeposited platinum on screen printed electrodes (Figure 9) show a clear increase in the amount of platinum on the surface as the number of cycles is increased from 5 (Figure 9A) to 100 (Figure 9E). Several important observations can be made from these images. First, it is important to note that the plain (unplatinized), screen printed electrode surface is quite rough with visible micron-scale carbon flakes. As the electrode is commercially produced by CH Instruments, its exact composition is proprietary; however, examination of Figure 9A shows a rough, nonuniform surface. The second observation that can be made is that the platinum appears to have deposited nonuniformly. This is not surprising, as it is known that defects in surface structure render a surface more electroactive.[45,55] Therefore, the electrodeposition did not occur evenly on the surface due to the uneven, rough surface of the as-purchased electrodes. The third observation to be noted is that the platinum deposition occurs only at existing platinum nanoparticles as the number of cycles exceeds 25 (Figure 9C); platinum nanoparticle size continues to increase with increasing current cycles.

Next, biosensor sensitivity data was examined in the context of the aforementioned observations. The response to glucose was recorded over four orders of magnitude (0-5 μM; 15-55 μM; 150-550 μM; and 1.5-5.5 mM) and the sensitivity of each prototype in the linear sensing range was calculated and plotted against the number of cycles of platinum deposition (Figure 10).

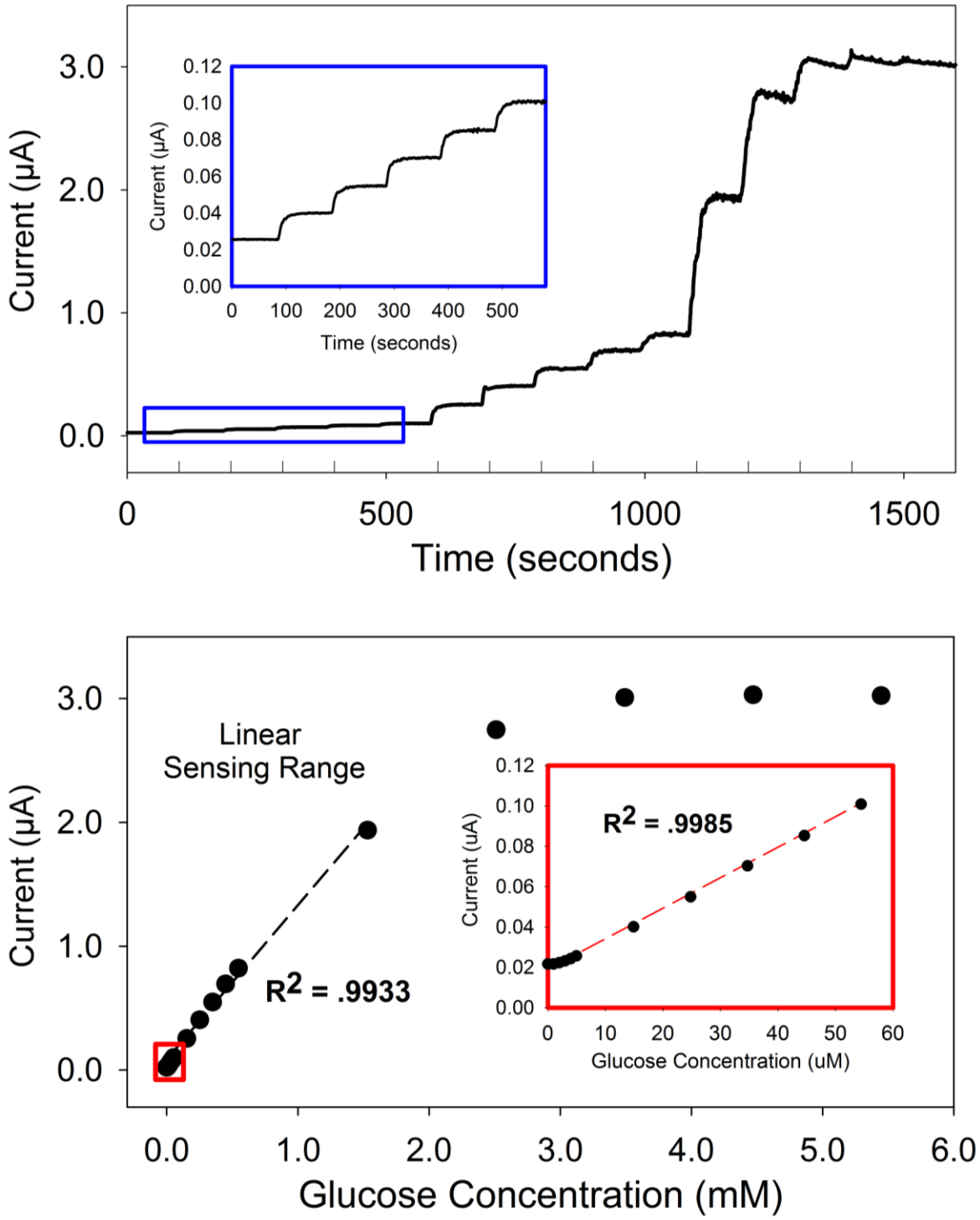

Figure 8. The top plot shows raw data obtained with glucose additions as a function of time. Beginning at a time adjusted to 100 seconds, 10 µL of glucose stock concentration 10 mM was added every 100 seconds. Beginning at 600 seconds, 100 mM glucose was added, and beginning at 1100 seconds, 1 M glucose was added.

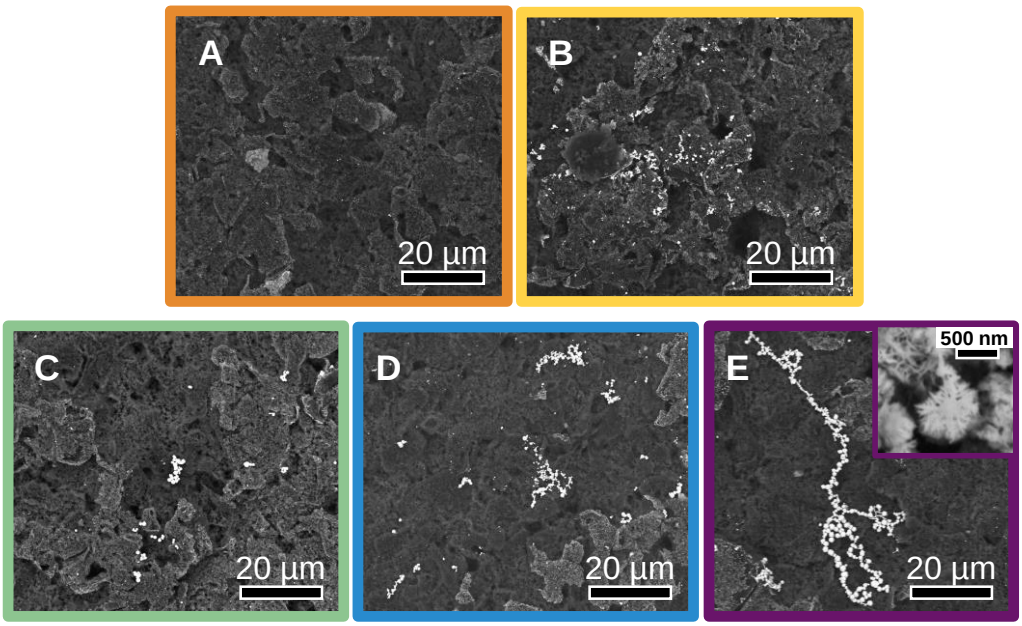

Figure 9. SEM images of platinum nanoparticles deposited on screen printed carbon electrodes. All deposition occurred at a current density of 7.12 mA/cm^2 following the procedure outlined in the "Methods" section. A) Electrode with 5 cycles of Pt deposition; B) 10 cycles of Pt deposition; C) 25 cycles; D) 50 cycles; E) 100 cycles. The inset of E) shows a close-up view of the deposited platinum nanostructures.

Results indicate that there is a significant increase in sensitivity with increasing platinum deposition to a certain point (25 cycles), but then increasing the concentration of platinum does not significantly improve the sensitivity (Figure 10). This result implies that when first-generation glucose biosensors are fabricated using platinum to decompose hydrogen peroxide, adding platinum will not continually improve sensor performance. Rather, a small amount of platinum is sufficient to decompose the hydrogen peroxide byproduct of the enzymatic binding. It is reasonable to conclude that platinum applied via electrodeposition at a current density of 7.12 mA/cm^2 will not affect the sensor performance when applied at cycles of more than 25. In fact, tests confirmed that the sensitivity of the studied glucose sensor reached a steady state value at platinum deposition cycles greater than 50.

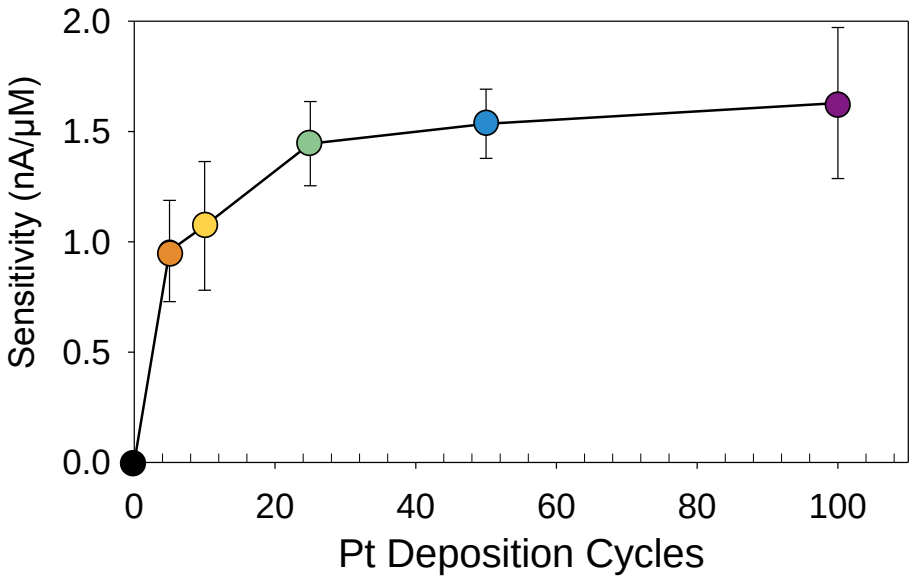

Figure 10. The average (n=3) sensitivity (nA/µM glucose) and corresponding standard deviation for sensors with varying amounts of platinum deposition. Sensors were prepared according to the procedure outlined in the "Methods" section.

This has potential implications on the usage of platinum in biosensors produced on a commercial scale. Two crucial components in the manufacturing process – raw material cost and duration of production – are both affected by the results from this study, as depositing platinum beyond the known beneficial amount of 25 cycles will not increase product performance due to peroxide decomposition but will, however, increase the product cost.

Conclusions

Platinum-based glucose biosensors have been in use for decades, yet limited information is available on the optimal deposition parameters for platinum nanoparticles applied via electrodeposition. Here we demonstrate that the relationship between applied platinum and biosensor sensitivity is not linear; rather, the sensor reaches a 'steady state' sensitivity above platinum deposition cycles of 50 or more. This information can be

applied in a cost analysis of platinum-based blood test strips or in other applications of the decomposition of hydrogen peroxide on platinum, such as underwater autonomous vehicles.[51,52] In order to validate these results, a future study should be conducted in which the current density of electrodeposition is a value other than 7.12 mA/cm^2. Then, the resulting 'maximum beneficial cycles' value could be compared to this work. There is a correlation between current density of deposition and sensor sensitivity towards hydrogen peroxide,[45] and while this study selected the known optimal current density, others should be investigated.

Acknowledgements

The authors greatly acknowledge support from the Iowa State University Department of Mechanical Engineering and College of Engineering.

CHAPTER 3: A WORKING ELECTRODE FOR SWEAT GLUCOSE MONITORING FABRICATED ENTIRELY VIA INKJET PRINTING

Introduction

The field of chemical biosensors, particularly glucose biosensors, has expanded tremendously in recent years as the number of diabetes mellitus diagnoses has increased in developing countries.[7,56] An illness affecting the production of insulin, diabetes requires daily management, which is often handled by patients directly.[4] The nature of the disease requires that patients monitor their blood glucose levels, a task that is most often accomplished through direct sampling. Direct blood sampling must be conducted intermittently throughout the day at an average frequency of three to four times daily[5] and provides the patient with a clear representation of his blood glucose levels, information he can then use to administer medication as needed. Though this process of direct blood sampling is relatively quick, usually taking just a few minutes, studies have shown that continuous monitoring can lead to a more accurate picture of blood glucose levels over extended periods of time.[5,10]

Continuous glucose monitoring can be achieved via sampling of many bodily fluids including blood, serum, sweat, tears, saliva, and interstitial fluid.[57] As the nature of continuous monitoring devices requires a constant physical interface with the patient, the accessibility of the sample medium is a key motivator in designing such a sensor. Consequently, sweat is a logical choice in sensing medium as its production rate can be easily affected by clothing, physical activity, and environmental conditions.[58] Sweat is also easily accessible, as activated sweat glands are located on the majority of the surface of the human body.[59] Another important factor is how well sweat glucose levels correlate

to blood glucose levels. Although additional studies need to be conducted, the literature indicates that sweat glucose concentration correlates to blood glucose concentration,[13] thus making it an acceptable medium to use for diabetic sensing requirements.

While wearable sweat glucose monitoring systems have been previously developed, they often require time-intensive and costly manufacturing processes such as clean room fabrication, photolithography, or metal sputtering. Numerous advanced manufacturing concepts hinge on additive manufacturing – creating an object by adding material – and one of the most well-known additive manufacturing processes is inkjet printing.[60] Inkjet printing has demonstrated applications in biosensing and is expected to significantly alter the landscape of mass-produced biosensors in the future.[61] It has also been demonstrated in other fields, including the development of solar cells,[62] photodetectors,[63] and drug delivery,[64] among others.

In this work we present the first entirely ink-jet printed working electrode for a glucose biosensor in three electrode format with functionality based on the decomposition of hydrogen peroxide catalyzed by platinum. Although glucose biosensors have been inkjet printed previously, they have either utilized sensing mechanisms that do not require platinum, or they are only partially inkjet printed, relying on other fabrication techniques for complete production (Table 2).

Methodology

Graphene electrode fabrication

Graphene electrodes – the base layer of the working electrode – were fabricated via inkjet printing with a Dimatix Materials Printer (Model DMP 2800, Fujifilm), as

previously published.[65] In short, single layer graphene powder (ACS Material GN1P0005) was dispersed in a mixture of 85% cyclohexanone (Sigma-Aldrich 398241) with 15% terpineol (Sigma-Aldrich T3407) via probe sonication for thirty minutes followed by bath sonication for several hours. The ink was filtered using a 0.8 µm syringe filter (GE Whatman), loaded into a 10 pL Dimatix printer cartridge, and printed on silicon wafers (Silicon Quest International). Sixty layers were printed with drop spacing of 20 µm, substrate temperature of 50°C, and cartridge temperature of 30°C. Electrodes were then thermally annealed under flowing nitrogen at 1000°C for 1 hour. Resistance measurements across the electrode after annealing were approximately 75 Ω.

Working electrode functionalization

The aforementioned thermally annealed graphene electrodes were used as the conductive base for the fabrication of the working electrode. The working electrode was created by inkjet printing four different inks on top of the graphene – insulating lacquer, platinum-decorated carbon nanotubes (Pt-CNTs), glucose oxidase, and glutaraldehyde.

The first layer printed, the insulating layer, served two purposes. First, it keeps the working area of the electrode constant. When an electrode is submerged in testing solution the lacquer leaves only a specific surface area exposed to solution, thus ensuring that each electrode tested has the same working surface area. Secondly, the insulating lacquer limits any wicking, thus any circuit shorting, that may occur as a result of extended testing in a liquid electrolyte solution. This ink was prepared on a volumetric basis with 75% cyclohexanone (Sigma-Aldrich 398241), 15% terpineol (Sigma-Aldrich T3407), and 10% acrylic lacquer (conventional nail polish), and printed at 40ºC.

As discussed in Chapter 2, platinum is an essential component of this sensor (Figure 6), as it decomposes the hydrogen peroxide byproduct of the glucose-glucose oxidase binding, which is the measurable signal detected by the biosensor. It is well known that platinum can be deposited via electrochemical deposition using applied current steps,[54] but as the objective of this project is to create an entirely inkjet-printable sensor, electrodeposition was eliminated as a possible deposition method. Instead, platinum nanoparticles (Sky Spring Nanomaterials 9410DX) were purchased and dispersed in a variety of solvents. However, the particles would not suspend in any combination of solvents tested at any relevant concentration and instead coagulated into visible clumps. As the 10 pL printer cartridge requires particle sizes less than 0.2 μm, it was determined that this ink could not be feasibly printed. In order to overcome the problem of dispersing the platinum nanoparticles in solution for inkjet printing, a commercially available platinum dispersion was purchased (Sigma Aldrich 773875, 3 nm particle size). It printed effectively but did not have a good response when five and 10 layer samples were tested with hydrogen peroxide. In an attempt to amplify the response, the number of layers printed was increased to 25 and then 50, but the resulting sensor still did not have the desired sensitivity. One reason for this is likely the morphology of the nanoparticles; the purchased suspension is believed to contain spherical nanoparticles, though it is well known that other morphologies such as leaves, petals, and cauliflower-like shapes are more effective for electrochemical sensing.[53,54] SEM images were taken in order to further investigate the platinum, but the captured images have very poor clarity and show charge accumulation on the surface, likely due to the solvents used to disperse the platinum nanoparticles, rendering them useless. These two problems – ineffective

nanoparticle morphology and charge accumulation due to solvents – deemed the platinum suspension ineffective.

Inkjet printing of carbon nanotubes has been previously demonstrated,[66,67] and our group has worked on attaching platinum nanoparticles to various substrates to achieve high loading in previous works,[45,51,52] so attaching platinum nanoparticles to carbon nanotubes and then printing the modified nanotubes was in the realm of possibility. Two methods were used to adhere platinum nanoparticles to carbon nanotubes, microwave-assisted deposition[68,69] and chemical deposition,[52] referred to herein as "microwave method" and "chemical method," respectively. Small batches of Pt-CNTs were prepared according to each method (Appendix), and then centrifuged with acetone to ensure that the acid was removed from the material before ink formulation, as the acid would affect pH which could in turn affect sensor performance.[70]

Each type of CNT was dispersed in two different solvents, sodium n-dodecyl sulfate (SDS) (Fisher BP166-100) and N,N-Dimethylformamide (DMF) (Sigma Aldrich 227056), to create four unique dispersions (Appendix). Each of the four inks was drop coated via pipette onto a screen printed carbon electrode (CH Instruments, SE101) and subsequently tested with hydrogen peroxide in a three electrode setup. Results (Figure 11) clearly indicate that the Microwave-SDS ink (top left) was ineffective, as only one current step is evident.

The Chemical-DMF ink (bottom right) can also be considered ineffective relative to the other results, as the signal is excessively noisy. Comparing the Chemical-SDS (top right) and Microwave-DMF (bottom left) results, the Microwave-DMF shows a higher

slope, indicating higher sensitivity, so it was selected as the final Pt-CNT ink to be used in the overall sensor fabrication.

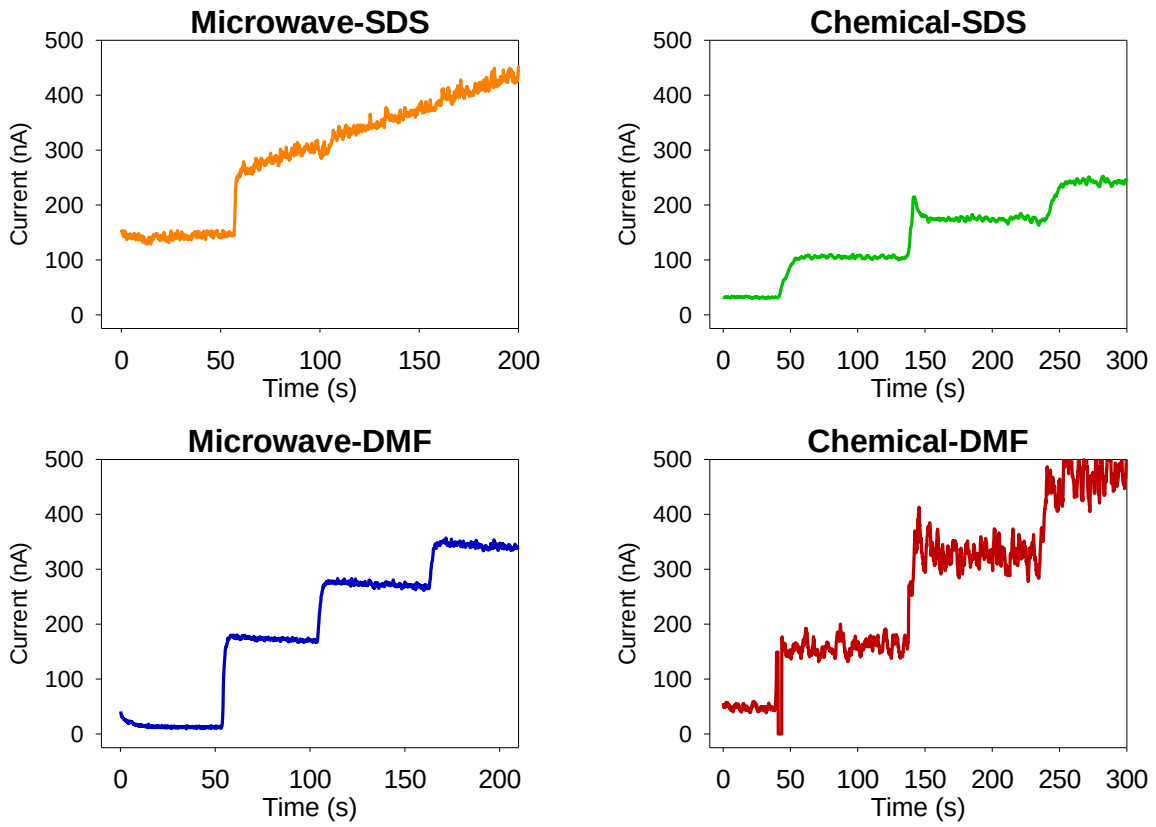

Figure 11. Each of the four Pt-CNT inks was drop coated on a screen printed carbon electrode and tested with hydrogen peroxide. The Microwave-DMF ink was determined to show the clearest signal with the highest sensitivity towards hydrogen peroxide.

The key finding of Chapter 2 – that platinum content does not improve performance of this specific sensing mechanism beyond a certain amount – was relevant in determining the number of layers of Pt-CNT ink to be printed. First, six layers and 12 layers were each printed on top of screen printed carbon electrodes. The rationale for such low numbers of layers was that the study in Chapter 2 utilized deposition cycles as low as five and 10. A mixture of GOx, BSA and glutaraldehyde was drop coated on top of the platinum layer and allowed to dry, and the sensor was evaluated for performance

by testing in a three electrode setup as outlined in Chapter 2. Results (Figure 12) show that there is little improved performance from six to 12 layers, but when the amount is increased approximately three-fold to 30 layers, performance improves significantly. Increasing platinum ink content to 50 and 100 layers did not show improvement, reinforcing conclusions from Chapter 2, so 30 layers was selected as the optimal amount of Pt-CNTs to be printed in the final sensor. To reiterate, these numbers of layers were selected for testing as they closely match the number of deposition cycles used in the study presented in Chapter 2.

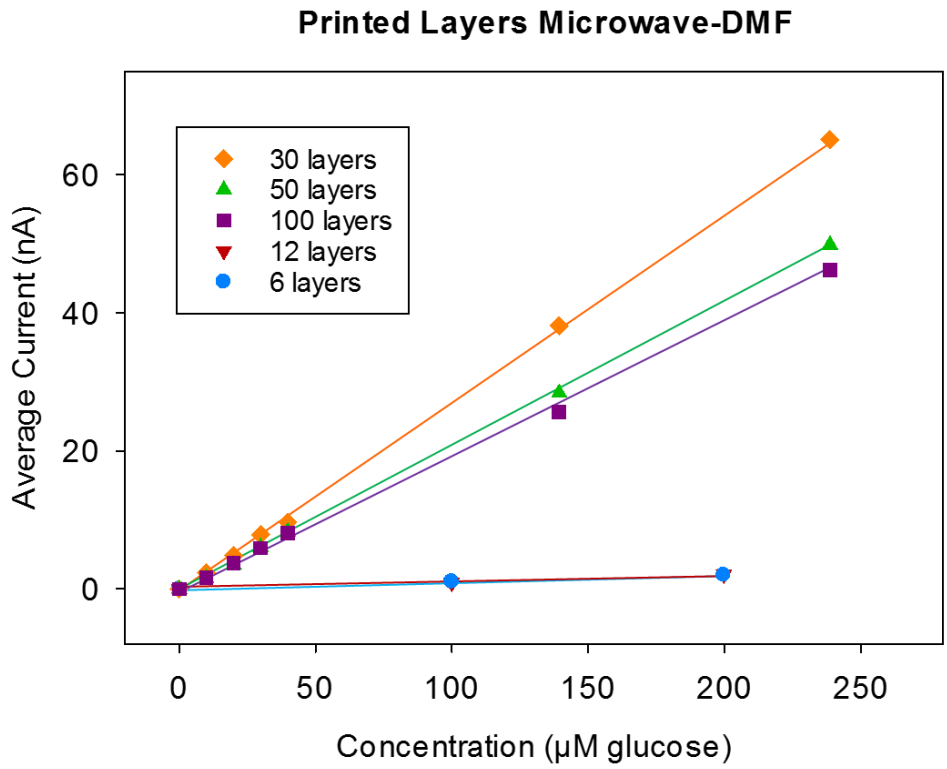

Figure 12. The number of layers of printed Pt-CNTs can significantly alter sensitivity. Thirty layers was selected for the final sensor.

Once the Pt-CNT ink composition and number of layers to be printed were determined, the enzymatic layer was investigated. Different sensors utilize varying concentrations of glucose oxidase enzyme, varying from 2 mg/mL to 20 mg/mL,[71-74]

without much explanation for selected concentration, so varying concentrations of glucose oxidase and BSA, a common stabilizing protein, were tested (Figure 13).[75] Please note that this was simply to find concentrations of enzyme and protein that functioned well; this was not a complete optimization or investigation, though the topic certainly could be.

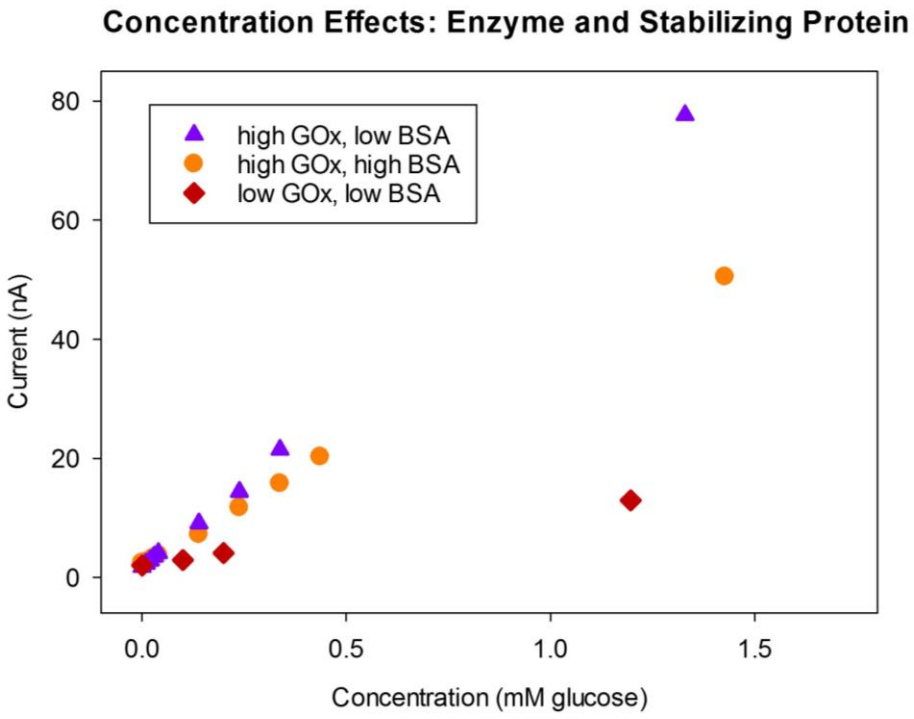

Figure 13. Varying concentrations of glucose oxidase and stabilizing protein BSA were investigated to determine an effective ratio. High GOx concentration refers to 20 mg/mL, low GOx refers to 8 mg/mL, low BSA refers to 80 mg/mL, high BSA refers to 160 mg/mL. All solutions were mixed in a 50/50 v/v ratio. BSA concentration 210 mg/mL was also tested, but caused the membrane to delaminate so the resulting electrode could not be tested.

The final component that needed to be inkjet printed was glutaraldehyde, which serves to chemically cross-link the enzyme to ensure that it does not dissolve in the test solution. The concentration of 2.5% was selected based on references in the literature.[75] Initially, the glutaraldehyde was mixed with the GOx-BSA solution and printed.

However, after just ten seconds of printing, the nozzles became clogged, which can be attributed to the fast-acting nature of glutaraldehyde cross-linking. Instead, the glucose oxidase mixture was printed first, and then glutaraldehyde was printed separately on top of that. This achieved the same result as printing the protein and cross-linker together, but ensured that the nozzle would not clog by the fast-acting glutaraldehyde.

Final electrode preparation protocol

A schematic outlining the various steps in preparing the inkjet printed working electrode is presented below (Figure 14). Graphene electrodes were prepared as described in the *Graphene electrode fabrication* subsection of Methodology section of this chapter (Figure 14 steps 1 and 2). An insulating lacquer layer was printed on top of the annealed graphene electrode to ensure that the surface area of the working electrode exposed in the electrolytic solution stayed constant (28.27 mm^2), and was allowed to dry at room temperature for thirty minutes (Figure 14 step 3). Next, 30 layers of the Pt-CNTs were printed and allowed to dry for six hours to ensure that all solvent was evaporated (Figure 14 step 4). Three layers of glucose oxidase dissolved in deionized water were printed in succession, and allowed to dry for one hour after the final layer was deposited (Figure 14 step 5). Finally, two layers of glutaraldehyde were printed to ensure cross-linking of the enzyme. The completed sensor was allowed to dry for at least thirty minutes prior to testing.

Experimental methodology

Experimental characterization was conducted using a traditional three electrode setup in 10 mL, 1X (10 mM) PBS, with the entirely inkjet printed sensor serving as the working electrode, a platinum wire as the counter, and a liquid Ag/AgCl reference

electrode. All electrochemical tests were carried out using a CH Instruments potentiostat (600E series) operating at an applied potential of +0.5 V. Stock solutions of glucose (1 mM, 10 mM, 100 mM and 1 M) were prepared using glucose (D-(+)-Glucose, Sigma Aldrich G8270) dissolved in PBS, and testing was conducted with a stir bar rotating at 725 rpm. Electrodes were allowed to stabilize for at least three minutes prior to data collection. Uric acid (Sigma-Aldrich U2625), ascorbic acid (Sigma-Aldrich A5960), lactic acid (Sigma-Aldrich W261106), sodium chloride (Sigma-Aldrich S7653) and potassium chloride (Sigma-Aldrich P9541) stock solutions were formulated by dissolving the respective target molecule in PBS.

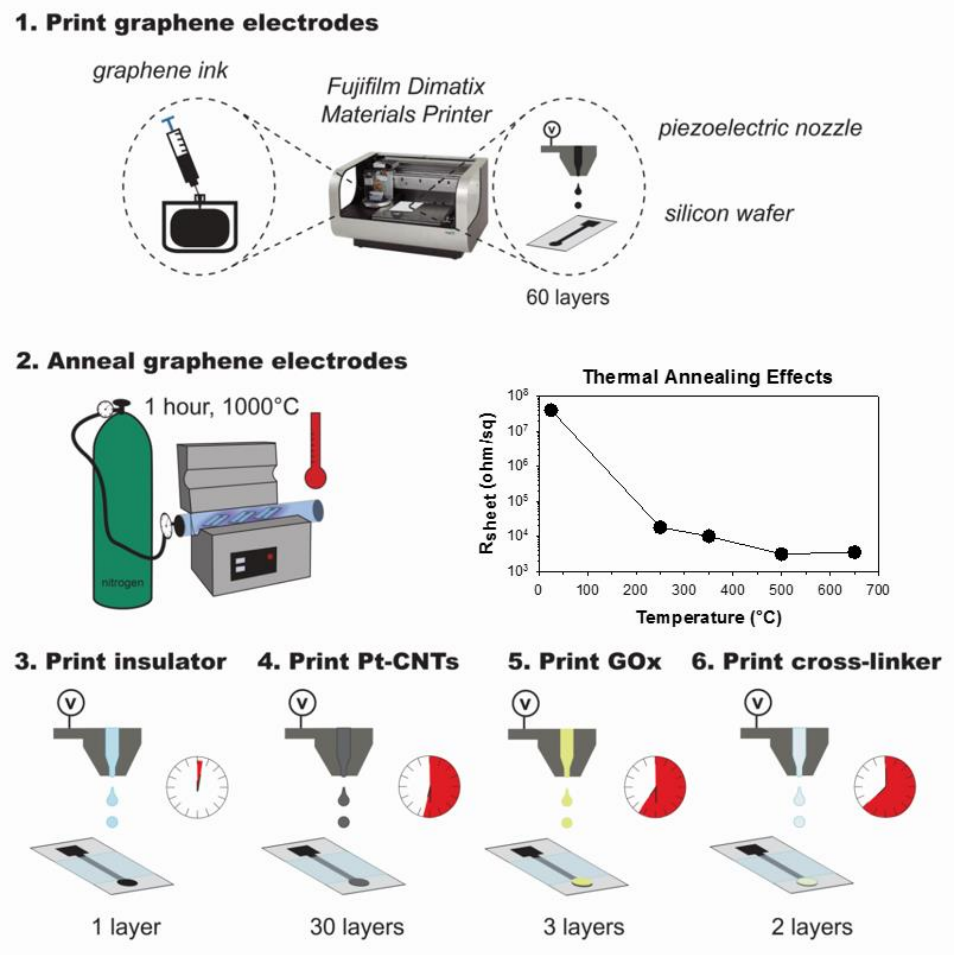

Figure 14. Schematic outlining the entire electrode fabrication process. Clocks between steps 3-6 indicate the total elapsed drying time for the entire process.

Results

Sensor characterization

Sensors were fabricated on four different days to ensure accuracy in manufacturing. Some were allowed to dry at room temperature for 24 hours prior to testing, while others were tested just two hours after the last fabrication step was completed. The sensors that were tested soon after production showed the best response, and thus they were selected for test data included in this manuscript. Figure 15 shows the raw data for one test using chronoamperometry at an applied potential of +0.5 V and the corresponding current vs. concentration plot with error bars representing ± one standard deviation. The current vs. concentration plot shows data points that represent an average current over a time interval of at least 20 seconds. Data was collected at a frequency of 0.1 seconds where each point represents an average of at least 200 data points.

The inkjet printed sensor showed an average sensitivity (slope) of 18.33 μA mM^{-1} cm^{-2}, average response time of 18 seconds to reach 90% of expected increased signal upon analyte (glucose) addition, experimental detection limit of 10 μm and theoretical detection limit of 3.79 μM glucose. Interestingly, the sensor showed current responses across four orders of magnitude of glucose concentrations. The potentiostat used in data acquisition only had the capability to capture precise data over three orders of magnitude during one test, so the full sensing range tests were run in two segments. The combined data is shown in Figure 16. The data from 10 μM to 2.51 mM has a coefficient of determination of 0.9975, indicating a highly linear correlation.

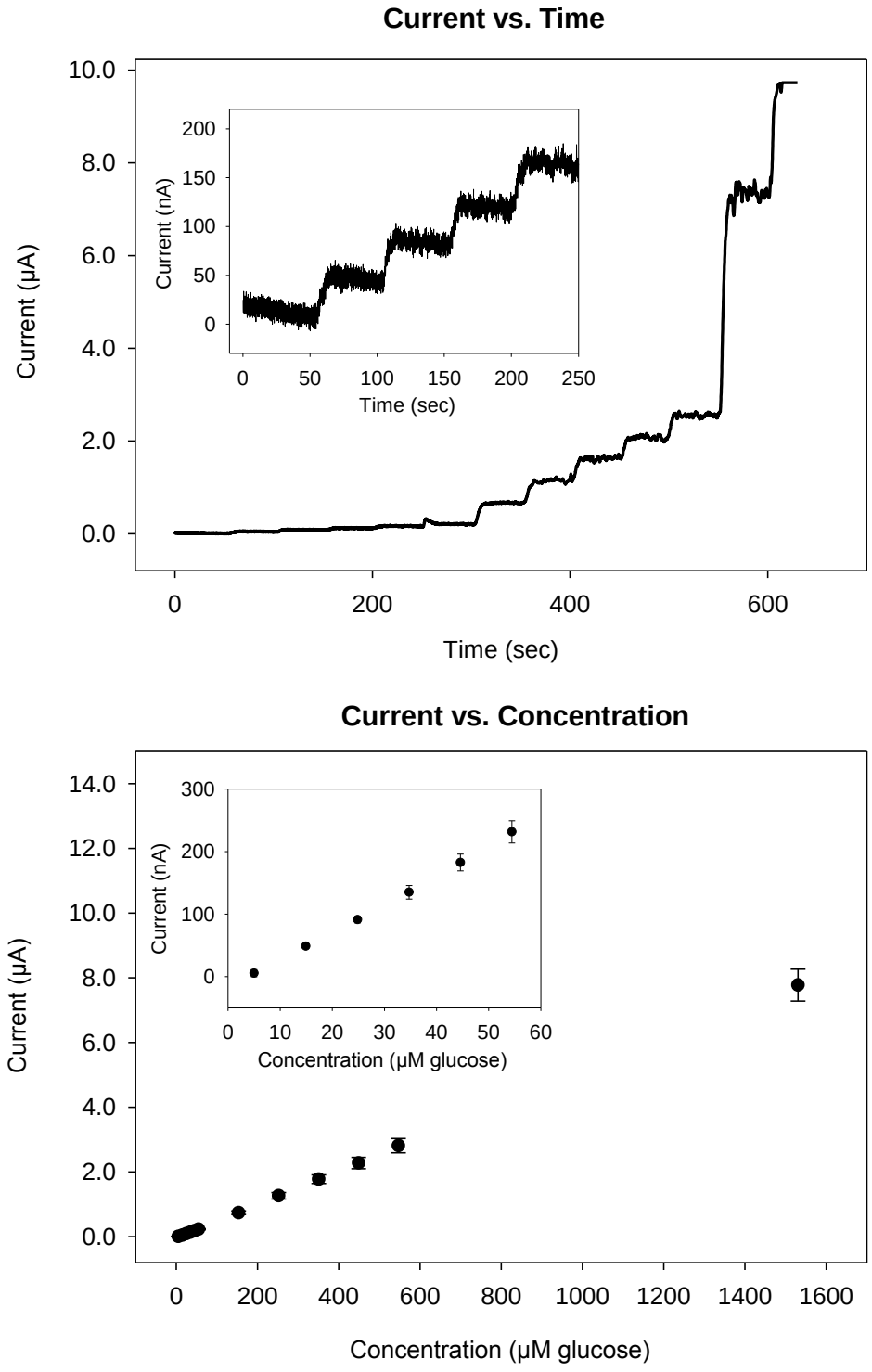

Figure 15. Sensor performance results for the entirely inkjet printed working electrode operating in a three electrode setup. The top plot displays the raw current vs. time data. Injections of 10 µL glucose were added every 50 seconds beginning at t=50 seconds. The first five additions were 10 mM glucose (inset), the second five were 100 mM glucose, and the final two before the current exceeded potentiostat limits were 1 M. The bottom figure displays the current response as a function of total solution glucose concentration. Error bars represent standard deviation for a sample size of three.

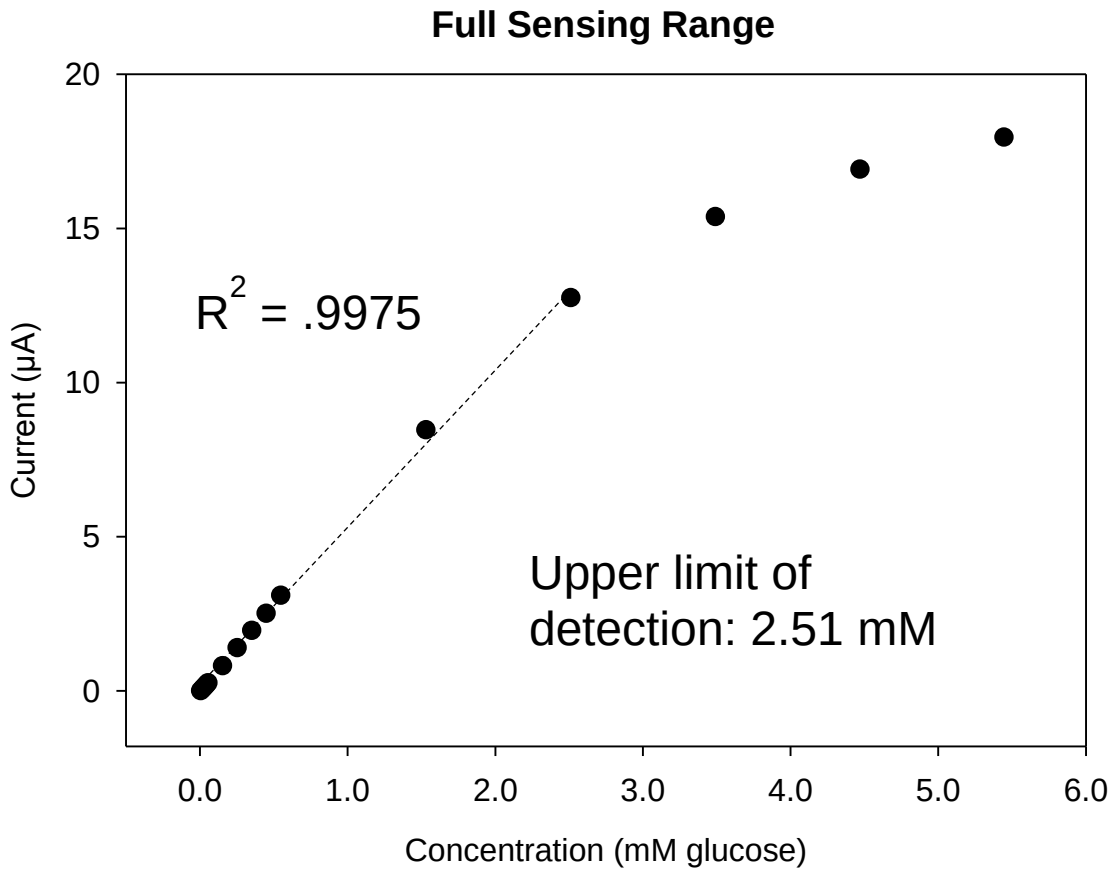

Figure 16. The full sensing range of the entirely inkjet printed glucose sensor. The current response is linear (correlation coefficient R^2 = .9975) from 10 μM to 2.51 mM glucose.

Stability

One key metric in evaluating biosensor performance is shelf life, often referred to as stability. Depending on the application of a biosensor, adequate shelf life can be as short as one day or as long as several years. Like many biosensors, this entirely inkjet printed working electrode showed a change in response as time went on, most notably in decreased sensitivity. While sensitivity is an important metric in biosensing, as long as a sensor maintains a linear region with clear current changes that can be correlated to substrate concentration changes, it can be calibrated and used effectively. However, if a sensor does not show reliable current increases, it cannot be trusted to give accurate readings.

Figure 17 displays response data from the sensor one day after fabrication and 10 days after fabrication. A clear difference can be seen in the resulting amperometric response. Not only does the 1-day-old sensor have a higher sensitivity, but the steps are explicit. In contrast, the 10-day-old sensor has a lower sensitivity and the steps are more difficult to distinguish, making it much less effective.

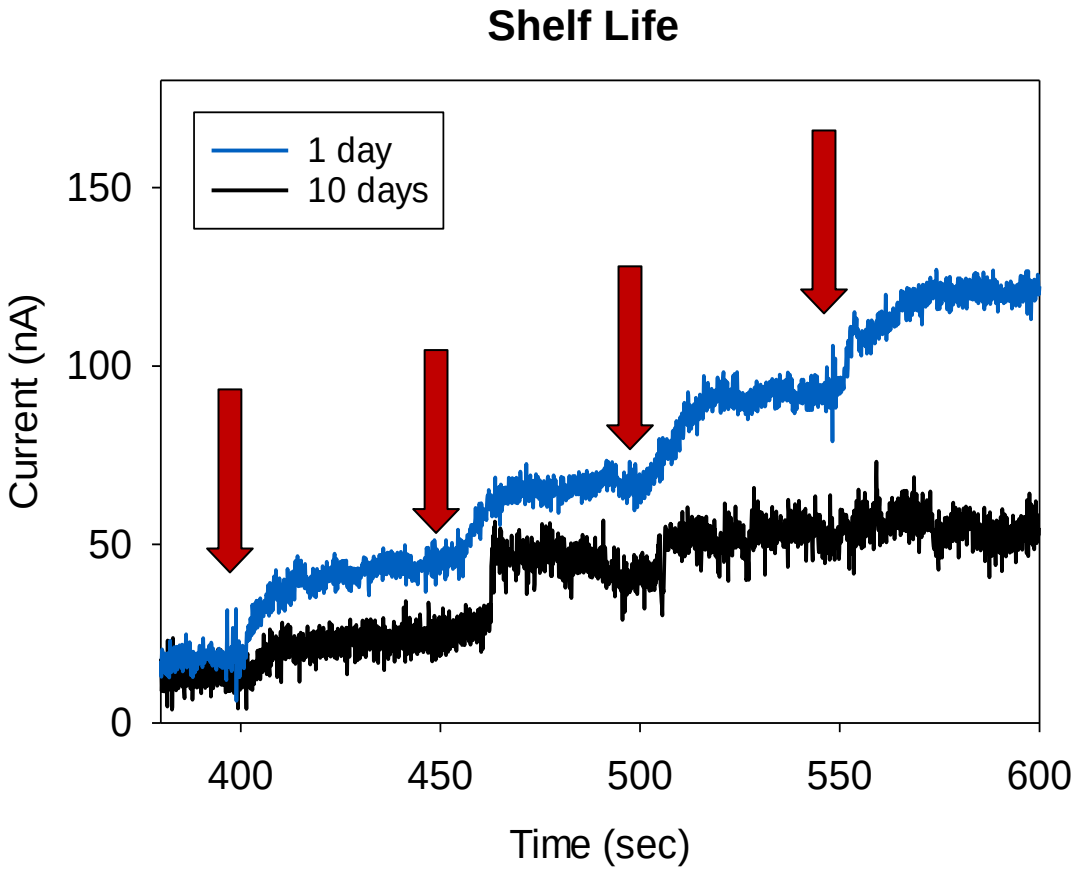

Figure 17. Raw data showing current responses to 10 μm increases in the total glucose concentration (red arrows correspond to time of injection). The blue line corresponds to a sensor that is 1 day old, while the black corresponds to a 10 day old sensor.

Interference data

One of the largest barriers in moving biosensors from the laboratory to the field is the response to interfering species. Oftentimes sensors in the laboratory are tested in pristine buffer solution, whereas in actuality real fluids, particularly biofluids, contain a multitude of components. Human sweat, for example, is known to contain over 61 different chemical constituents.[12] In order for a biosensor to be effective it must be able to selectively sense the target analyte; that is, produce a signal that corresponds to the concentration of target analyte *only*, and not respond to changes in concentration of any other chemical. There are two key categories of potential interfering species used in this study: electrolytes and acids. The electrolytes studied include NaCl, Na_2SO_4, $NaHCO_3$, KCl, $MgCl_2$, NaH_2PO_4 , $CaCO_3$ and NH_4Cl,[12] while the acids studied include uric acid, lactic acid, and ascorbic acid, three acids commonly used in interference testing of glucose biosensors.[12,22]

The influence of electrolytes on the sensor performance was studied by testing the sensor in an artificial sweat solution rather than pristine PBS. The artificial sweat used comprised the aforementioned electrolytes in physiologically comparable concentrations,[12] dissolved in deionized water. In order to understand the impact of electrolytes, an amperometric test was run first in PBS then in artificial sweat, and the results compared (Figure 18). The sensitivity decreases by 87% when the sensor operates in artificial sweat, which is a significant change. However, it is important to note that although the magnitude of the response has decreased, it is still extremely linear. This linearity, described quantitatively with a correlation coefficient of 0.9997, is still

extremely high, meaning that the sensor could still effectively correlate current to sweat glucose concentration.

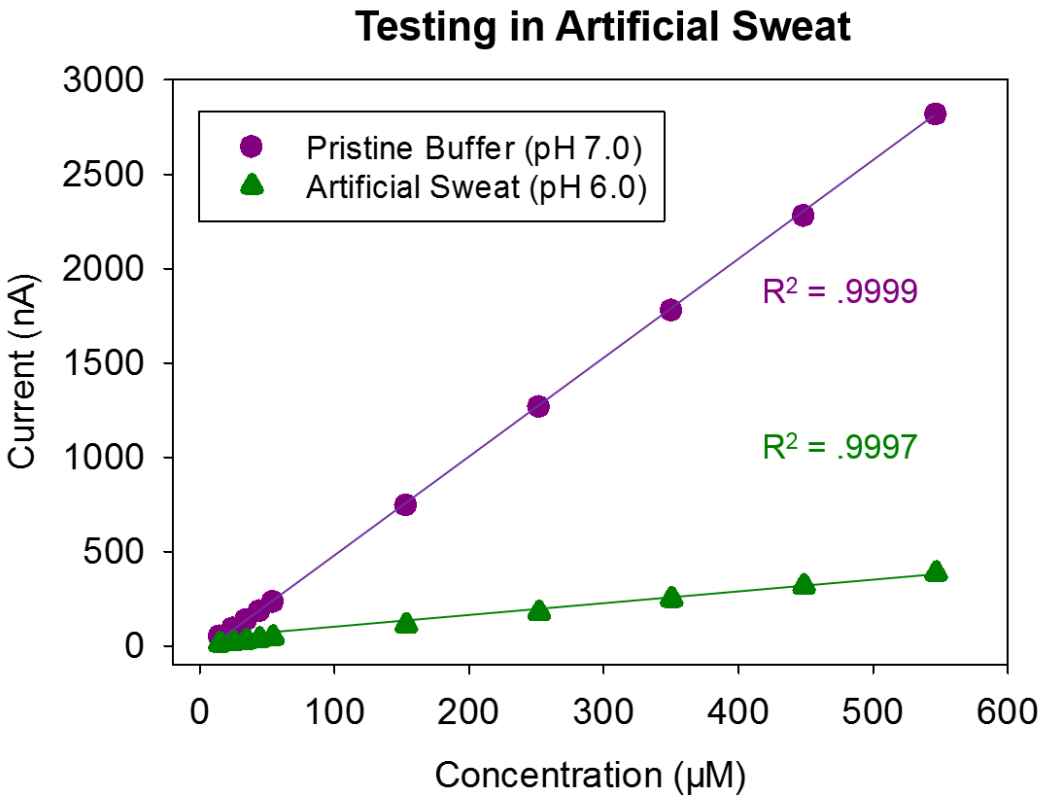

Figure 18. Current response vs. concentration glucose in pristine buffer solution (purple) and artificial sweat (green).

While a sensor must operate in a constant background of potentially interfering species, it is also important to understand how sudden changes in concentration of a particular analyte can affect performance. In particular, glucose biosensors are often tested this way against acids.[22,45] In this study, NaCl, KCl, uric acid, lactic acid, and ascorbic acid, relevant interfering species found in human sweat, were tested by spiking testing solution with each component individually to a final concentration corresponding to the physiological concentration found in sweat. Concentrations used in this study are as follows: 25 mM NaCl, 10 mM KCl, 60 µM uric acid, 14 mM lactic acid, and 10 mM

ascorbic acid.[12] A completed (enzyme functionalized and cross-linked), entirely printed electrode was tested, along with an electrode that only contained 30 layers printed Pt-CNTs on annealed graphene (no enzyme), in order to observe what effect the presence of enzyme may have on the response (Figure 19). Note that the spikes in current that occur at each injection are the result of the physical injection, which disrupts the steady state of the system. Two observations occurred as expected. First, that the addition of glucose affected only the current response of the sensor functionalized with glucose oxidase, and second that the magnitude of the response to glucose decreased in the presence of interfering species. That is, the current response to injection g (time = 410 seconds) is much smaller than the equivalent concentration increase at injection a (time = 100 seconds), even though both are well within the upper limit of the linear range (2.5 mM).

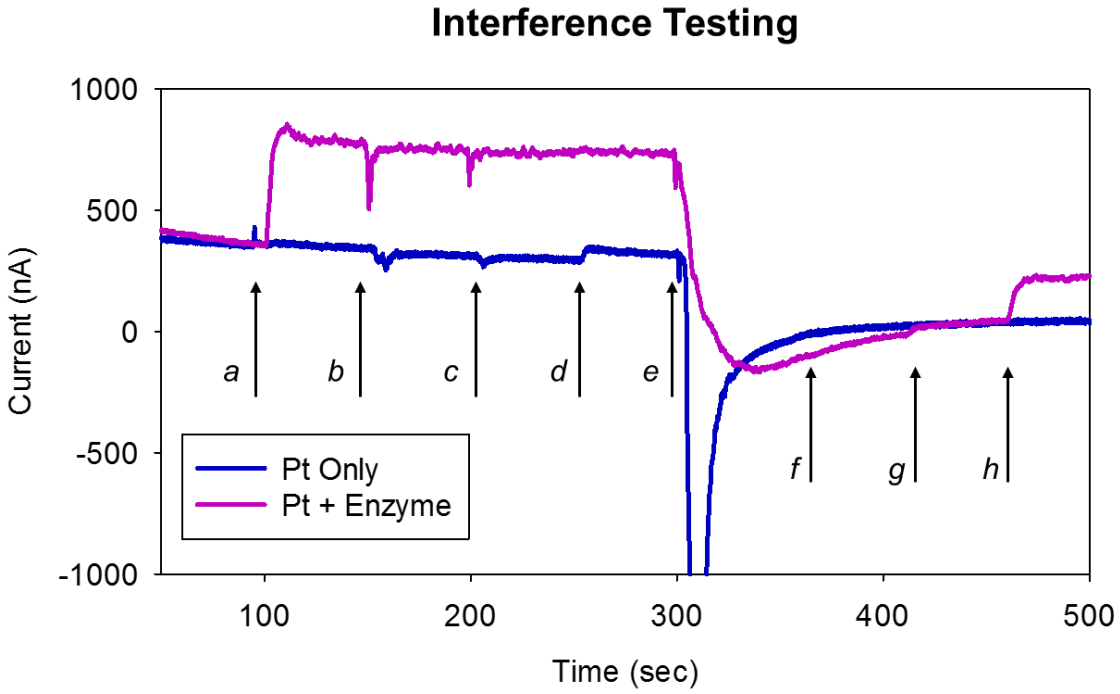

Figure 19. Amperometric current vs. time data obtained at an opeating potential of +0.5 V with a stir bar rotating at 725 rpm. Arrows correspond to the injection of analyte to produce a final concentration as follows: a) 0.1 mM glucose; b) 25 mM NaCl; c) 10 mM KCl; d) 60 μM uric acid; e) 14 mM lactic acid; f) 10 mM ascorbic acid; g) 0.2 mM glucose; h) 1.2 mM glucose.

The most notable change in current occurs after injection e (time = 300 seconds), which corresponds to the addition of lactic acid to the system. Interestingly, the response is seen in both the enzymatic electrode and the Pt-CNT only electrode, but the magnitude of the response is greater for the enzymatic working electrode. This could be due to the change in pH of the system upon the addition of this acid, an effect of the lactic acid itself with the Pt-CNTs, or possibly an effect of the three acids combined. Further testing must be done in order to draw conclusions regarding this current response.

Discussion

The developed sensor demonstrates adequate detection limit, linear range, response time, and shelf life for applications in a wearable sweat-based glucose sensor. Importantly, this sensor functions well not only in PBS but also in synthetic sweat, indicating that it has potential for use outside of a laboratory environment. Aspects of this sensor that should be further investigated include the impact of additional interfering species, the performance of the sensor over extended periods of time, and how different storage conditions impact performance, and are discussed further in Chapter 4.

Table 2 contains a summary of all the glucose biosensors that have been inkjet printed, many of which are colorimetric rather than electrochemical. It is interesting to note that the oldest reference found was from 1992 – though glucose sensors have been around for a long time, inkjet printing is a relatively new concept. Most of the references from recent years utilize the same Fujifilm Dimatix Materials Printer 2800 that is used in this work. It should also be noted that none of the inkjet printed sensors utilize the

platinum-decomposition reaction that is the core of this thesis. This work is, to our knowledge, the first time such a scheme has been entirely inkjet printed.

Table 2. A summary of the inkjet printed glucose sensors demonstrated in the literature. *Colorimetric sensing basis

Printing Completeness	Inkjet Printer	Ink(s)	Substrate	Additional Processes	Linear Response Range	Operating Potential	Ref
Partially	Thermal Canon inkjet printer (i905D)	Biological ink: GOx in PBS with EDTA and glycerol PEDOT/PSS and Tween 80	ITO-coated glass	Dip coating	20-60 mM	+.6 V, +.3 V	72
Partially	Dimatix piezoelectric inkjet	Working electrode ink (nonenzymatic sensor): CuO-NPs deionized water, ethanol, isopropyl alcohol, ethylene glycol	Si/Ag	Sputtering, microwave -assisted annealing	0.05-18.45 mM	+.6 V	76
Partially	Dimatix Materials Printer 2800	Glucose oxidase, pyrrole, PBA, Gemini surfactant, FepTS, $FeCl_3$. Then printed layer of 0.5% w/v ethyl cellulose in butanol	Screen printed carbon electrodes	No	1-5 mM	+.6 V	71
Entirely	Microjet PicoJet-2000	340 units of GOx, 136 units of HRP in 10 mL citrate buffer mixed with 7.5 mg o-toluidine dissolved in 10 mL of ethanol in a 1:1 volume ratio, 0.075 wt % sodium L-ascorbate dissolved in the obtained solution	Filter paper soaked in 1.0 wt% solution of poly(styrene) in toluene	No	2.8-28.0 mM	N/A*	77*
Partially	Dimatix Materials Printer 2800	Water, GOx, HRP, PEDOT-PSS	ITO-coated PET film	Dip coating in acetone	1.44 mM to .59 M	+.3 V	78
Partially	Ink-Jet printer (Biodot, UK)	Tetrathiafulvalene (TTF) in ethanol (0.05% w/v), Tetrabutylammonium perchlorate (l% w/v), GOx in PBS (0.05% w/v), BSA in PBS (0.05% w/v), glutaraldehyde in PBS (5% w/v)	Screen printed carbon electrodes	No	1-6 mM	Not provided	79
Entirely	Epson ME1+ piezoelectric ink-jet printer	HRP and GOx ink: enzyme solution (1 mg/mL) in PBS, 140 mg/mL of tert-butanol and 23 mg/mL of PEG-20000	Photo paper, parchment paper	No	0-20 mM	N/A*	80*
Partially	In-house designed lab printer	20 mg/mL GOx with PBS, 5% (w/v) glycerol added as a stabilizer	Screen printed carbon black electrodes	No	Not tested	Not tested	73

CHAPTER 4

CONCLUSIONS AND FUTURE PERSPECTIVES

In summary, this work has demonstrated an entirely inkjet printed working electrode for use in sweat-based, continuous wearable glucose monitoring. This project brings together research focuses in advanced manufacturing, nanomaterials, and wearable technology to create a sensor that shows promise in revolutionizing the way diabetics monitor and treat their disease. Moving towards noninvasive, continuous monitoring will enable diabetics to monitor their disease in a way which requires less effort but offers a more complete view of their glucose levels.

This work was focused equally on the development and characterization of an enzymatic glucose sensor. While Chapter 3 gives a thorough explanation for how and why each component of the sensor was developed, additional work can and should be done to further understand the performance of this sensor. Specifically, additional tests should be run to understand the effect of different interfering constituents. Though certain analytes were tested (Figure 19), to what extent the resulting current changes can be attributed to each specific analyte requires further investigation. For example, acidic analytes should be tested individually over extended time periods, and also sequentially in varying orders of addition to see if certain combinations impact the response. This study examined only a small percentage of potential interfering species. Not only does sweat comprise over 60 chemical constituents, but a variety of additional components (ie. dirt, fragrance, moisturizers) can be found on the skin and could contaminate the sweat before it contacts the sensor.

The next step in pushing this inkjet printed sensor from the laboratory to commercialization is to fabricate it on a flexible substrate. A silicon wafer was selected for this work as it can withstand the high temperatures required for thermally annealing the graphene ink, but the Claussen Lab is currently working to install laser annealing facilities at Iowa State University. A laser annealing process has been shown to effectively transform the surface of the inkjet printed graphene into a conductive structure that is electrochemically effective.[65] The laser annealing process eliminates the need for a high temperature environment, thus making it possible to create these conductive graphene electrodes on a variety of substrates such as polyimide film, glass, and even fabric. Every subsequent step mentioned in Chapter 3 could be inkjet printed on a flexible substrate just as easily as it could be on silicon, though some printing parameters would need to be reoptimized. Inkjet printing on a flexible substrate is of significant interest, as it could be scaled up to a roll-to-roll process that would allow for inexpensive manufacturing (Figure 20).

The scalable nature of inkjet printing makes it an extremely attractive manufacturing process, and in order to make this wearable sensor a reality the counter and reference electrode should be inkjet printed, too. The platinum wire used in this work for the counter could be easily replaced by a conductive graphene electrode, but printing the Ag/AgCl reference would be difficult. Developing a reference ink that can be inkjet printed without the need for high temperature annealing or other post-print processing would make this wearable sensor even more realistic.

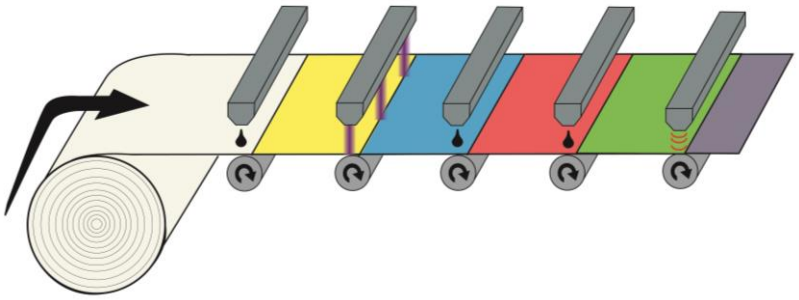

Figure 20. An entirely inkjet printed sensor developed on flexible substrate has the potential to be effectively scaled up to mass manufacture on a roll-to-roll system. This figure illustrates the principle and potential of this method.

Regarding wearable sensors, public interest has surged in recent years, and with the expected increase of diseases that require daily monitoring such as diabetes, the market for wearable sensors is expected to expand drastically in the next ten years. Platforms currently in existence such as the Apple Watch® require the user to actively attach a piece of equipment, which can be cumbersome and unsightly. However, if researchers and designers are able to work together to create sensors that are integrated into clothing or garments that people already wear, the appeal of such sensors would increase. In conclusion, inkjet printing is anticipated to become a fairly common manufacturing method particularly in the realm of products integrating nanomaterials as it is relatively simple, low cost, and can be conducted with a variety of materials and on a variety of substrates.

REFERENCES

1. Turner, A. P. F. (2013). Biosensors: sense and sensibility. *Chemical Society Reviews, 42*(8), 3184-3196. doi:10.1039/C3CS35528D

2. Koyun, A., Ahlatcolu, E., Koca, Y., & Kara, S. (2012). Biosensors and their principles. *A Roadmap of Biomedical Engineers and Milestones*.

3. Services, U. S. D. o. H. a. H. (2014). Centers for Disease Control and Prevention. National Diabetes Statistics Report: Estimates of Diabetes and Its Burden in the United States.

4. Toobert, D. J., Hampson, S. E., & Glasgow, R. E. (2000). The summary of diabetes self-care activities measure: results from 7 studies and a revised scale. *Diabetes Care, 23*(7), 943-950. doi:10.2337/diacare.23.7.943

5. Klonoff, D. C. (2005). Continuous Glucose Monitoring. *Roadmap for 21st century diabetes therapy, 28*(5), 1231-1239. doi:10.2337/diacare.28.5.1231

6. Guariguata, L., Whiting, D. R., Hambleton, I., Beagley, J., Linnenkamp, U., & Shaw, J. E. (2014). Global estimates of diabetes prevalence for 2013 and projections for 2035. *Diabetes Research and Clinical Practice, 103*(2), 137-149. doi:http://dx.doi.org/10.1016/j.diabres.2013.11.002

7. Newman, J. D., & Turner, A. P. F. (2005). Home blood glucose biosensors: a commercial perspective. *Biosensors and Bioelectronics, 20*(12), 2435-2453. doi:http://dx.doi.org/10.1016/j.bios.2004.11.012

8. Hughes, M. D. (2009). The Business of Self-Monitoring of Blood Glucose: A Market Profile. *Journal of Diabetes Science and Technology, 3*(5), 1219-1223. doi:10.1177/193229680900300530

9. Clarke, S. F., & Foster, J. R. (2012). A history of blood glucose meters and their role in self-monitoring of diabetes mellitus. *British journal of biomedical science, 69*(2), 83-93. Retrieved from http://europepmc.org/abstract/MED/22872934

10. Salardi, S., Zucchini, S., Santoni, R., Ragni, L., Gualandi, S., Cicognani, A., & Cacciari, E. (2002). The Glucose Area Under the Profiles Obtained With Continuous Glucose Monitoring System Relationships With HbAlc in Pediatric Type 1 Diabetic Patients. *Diabetes Care, 25*(10), 1840-1844. doi:10.2337/diacare.25.10.1840

11. Chen, C., Xie, Q., Yang, D., Xiao, H., Fu, Y., Tan, Y., & Yao, S. (2013). Recent advances in electrochemical glucose biosensors: a review. *RSC Advances, 3*(14), 4473-4491. doi:10.1039/C2RA22351A

12. Harvey, C. J., LeBouf, R. F., & Stefaniak, A. B. (2010). Formulation and stability of a novel artificial human sweat under conditions of storage and use. *Toxicology in Vitro, 24*(6), 1790-1796. doi:http://dx.doi.org/10.1016/j.tiv.2010.06.016

13. Moyer, J., Wilson, D., Finkelshtein, I., Wong, B., & Potts, R. (2012). Correlation Between Sweat Glucose and Blood Glucose in Subjects with Diabetes. *Diabetes Technology & Therapeutics, 14*(5), 398-402. doi:10.1089/dia.2011.0262

14. Sato, K., Kang, W. H., Saga, K., & Sato, K. T. (1989). Biology of sweat glands and their disorders. I. Normal sweat gland function. *Journal of the American Academy of Dermatology, 20*(4), 537-563. doi:http://dx.doi.org/10.1016/S0190-9622(89)70063-3

15. Al-Tamer, Y., & Hadi, E. (1994). Age dependent reference intervals of glucose, urea, protein, lactate and electrolytes in thermally induced sweat. *Clinical Chemistry and Laboratory Medicine, 32*(2), 71-78.

16. Emrich, H., Stoll, E., Friolet, B., Colombo, J., Richterich, R., & Rossi, E. (1968). Sweat composition in relation to rate of sweating in patients with cystic fibrosis of the pancreas. *Pediatric research, 2*(6), 464-478.

17. Boyne, M. S., Silver, D. M., Kaplan, J., & Saudek, C. D. (2003). Timing of Changes in Interstitial and Venous Blood Glucose Measured With a Continuous Subcutaneous Glucose Sensor. *Diabetes, 52*(11), 2790-2794. doi:10.2337/diabetes.52.11.2790

18. Thomé-Duret, V., Reach, G., Gangnerau, M. N., Lemonnier, F., Klein, J. C., Zhang, Y., . . . Wilson, G. S. (1996). Use of a Subcutaneous Glucose Sensor To Detect Decreases in Glucose Concentration Prior to Observation in Blood. *Analytical Chemistry, 68*(21), 3822-3826. doi:10.1021/ac960069i

19. Oliver, N. S., Toumazou, C., Cass, A. E. G., & Johnston, D. G. (2009). Glucose sensors: a review of current and emerging technology. *Diabetic Medicine, 26*(3), 197-210. doi:10.1111/j.1464-5491.2008.02642.x

20. Chatterjee, P. R., De, S., Datta, H., Chatterjee, S., Biswas, M. C., Sarkar, K., & Mandal, L. K. (2003). Estimation of tear glucose level and its role as a prompt indicator of blood sugar level. *Journal of the Indian Medical Association, 101*(8), 481-483. Retrieved from http://europepmc.org/abstract/MED/15071801

21. Alexeev, V. L., Das, S., Finegold, D. N., & Asher, S. A. (2004). Photonic Crystal Glucose-Sensing Material for Noninvasive Monitoring of Glucose in Tear Fluid. *Clinical Chemistry, 50*(12), 2353-2360. doi:10.1373/clinchem.2004.039701

22. Gao, W., Emaminejad, S., Nyein, H. Y. Y., Challa, S., Chen, K., Peck, A., . . . Javey, A. (2016). Fully integrated wearable sensor arrays for multiplexed in situ perspiration analysis. *Nature, 529*(7587), 509-514. doi:10.1038/nature16521

23. Burtis, C., & Ashwood, E. (1999). Tietz textbook of clinical chemistry.

24. Flattau, P. E., & Conditions, N. R. C. W. G. o. C. L. U. U. A. (1991). Environmental Conditions and Tear Chemistry.

25. Yamaguchi, M., Mitsumori, M., & Kano, Y. (1998). Noninvasively measuring blood glucose using saliva. *Engineering in Medicine and Biology Magazine, IEEE, 17*(3), 59-63.

26. Glasstone, S. (2013). *An introduction to electrochemistry*: Read Books Ltd.

27. Bioanalytical Systems, I. (2016). Reference Electrodes.

28. Zhang, S., Wright, G., & Yang, Y. (2000). Materials and techniques for electrochemical biosensor design and construction. *Biosensors and Bioelectronics, 15*(5–6), 273-282. doi:http://dx.doi.org/10.1016/S0956-5663(00)00076-2

29. Claussen, J. C. (2016). ME 550X: Advanced Biosensors [Class lecture slides].

30. Rohan. (2015). Biosensors Market worth $22.68 Billion by 2020 [Press release]. Retrieved from http://www.marketsandmarkets.com/PressReleases/biosensors.asp

31. Association, A. D. (2011). Standards of Medical Care in Diabetes—2011. *Diabetes Care, 34*(Supplement 1), S11-S61. doi:10.2337/dc11-S011

32. Bandodkar, A. J., Molinnus, D., Mirza, O., Guinovart, T., Windmiller, J. R., Valdés-Ramírez, G., . . . Wang, J. (2014). Epidermal tattoo potentiometric sodium sensors with wireless signal transduction for continuous non-invasive sweat monitoring. *Biosensors and Bioelectronics, 54*, 603-609. doi:http://dx.doi.org/10.1016/j.bios.2013.11.039

33. Kudo, H., Sawada, T., Kazawa, E., Yoshida, H., Iwasaki, Y., & Mitsubayashi, K. (2006). A flexible and wearable glucose sensor based on functional polymers with Soft-MEMS techniques. *Biosensors and Bioelectronics, 22*(4), 558-562. doi:http://dx.doi.org/10.1016/j.bios.2006.05.006

34. Jina, A., Tierney, M. J., Tamada, J. A., McGill, S., Desai, S., Chua, B., . . . Christiansen, M. (2014). Design, Development, and Evaluation of a Novel Microneedle Array-based Continuous Glucose Monitor. *Journal of Diabetes Science and Technology, 8*(3), 483-487. doi:10.1177/1932296814526191

35. Bandodkar, A. J., Jia, W., Yardımcı, C., Wang, X., Ramirez, J., & Wang, J. (2015). Tattoo-Based Noninvasive Glucose Monitoring: A Proof-of-Concept Study. *Analytical Chemistry, 87*(1), 394-398. doi:10.1021/ac504300n

36. Wang, J. (2008). Electrochemical Glucose Biosensors. *Chemical Reviews, 108*(2), 814-825. doi:10.1021/cr068123a

37. Wang, J. (2001). Glucose Biosensors: 40 Years of Advances and Challenges. *Electroanalysis, 13*(12), 983-988. doi:10.1002/1521-4109(200108)13:12<983::AID-ELAN983>3.0.CO;2-#

38. Wang, J. (2005). Carbon-Nanotube Based Electrochemical Biosensors: A Review. *Electroanalysis, 17*(1), 7-14. doi:10.1002/elan.200403113

39. Taguchi, M., Ptitsyn, A., McLamore, E. S., & Claussen, J. C. (2014). Nanomaterial-mediated Biosensors for Monitoring Glucose. *Journal of Diabetes Science and Technology, 8*(2), 403-411. doi:10.1177/1932296814522799

40. Rick, J., Tsai, M.-C., & Hwang, B. (2016). Biosensors Incorporating Bimetallic Nanoparticles. *Nanomaterials, 6*(1), 5. Retrieved from http://www.mdpi.com/2079-4991/6/1/5

41. Wu, H., Wang, J., Kang, X., Wang, C., Wang, D., Liu, J., . . . Lin, Y. (2009). Glucose biosensor based on immobilization of glucose oxidase in platinum nanoparticles/graphene/chitosan nanocomposite film. *Talanta, 80*(1), 403-406. doi:http://dx.doi.org/10.1016/j.talanta.2009.06.054

42. Cui, H.-F., Ye, J.-S., Zhang, W.-D., Li, C.-M., Luong, J. H. T., & Sheu, F.-S. (2007). Selective and sensitive electrochemical detection of glucose in neutral solution using platinum–lead alloy nanoparticle/carbon nanotube nanocomposites. *Analytica Chimica Acta, 594*(2), 175-183. doi:http://dx.doi.org/10.1016/j.aca.2007.05.047

43. Qu, F., Yang, M., Shen, G., & Yu, R. (2007). Electrochemical biosensing utilizing synergic action of carbon nanotubes and platinum nanowires prepared by template synthesis. *Biosensors and Bioelectronics, 22*(8), 1749-1755. doi:http://dx.doi.org/10.1016/j.bios.2006.08.003

44. Zou, Y., Xiang, C., Sun, L.-X., & Xu, F. (2008). Glucose biosensor based on electrodeposition of platinum nanoparticles onto carbon nanotubes and immobilizing enzyme with chitosan-SiO2 sol–gel. *Biosensors and Bioelectronics, 23*(7), 1010-1016. doi:http://dx.doi.org/10.1016/j.bios.2007.10.009

45. Claussen, J. C., Kumar, A., Jaroch, D. B., Khawaja, M. H., Hibbard, A. B., Porterfield, D. M., & Fisher, T. S. (2012). Nanostructuring Platinum Nanoparticles on Multilayered Graphene Petal Nanosheets for Electrochemical Biosensing. *Advanced Functional Materials, 22*(16), 3399-3405. doi:10.1002/adfm.201200551

46. Claussen, J. C., Hengenius, J. B., Wickner, M. M., Fisher, T. S., Umulis, D. M., & Porterfield, D. M. (2011). Effects of Carbon Nanotube-Tethered Nanosphere Density on Amperometric Biosensing: Simulation and Experiment. *The Journal of Physical Chemistry C, 115*(43), 20896-20904. doi:10.1021/jp205569z

47. McLamore, E. S., Shi, J., Jaroch, D., Claussen, J. C., Uchida, A., Jiang, Y., . . . Porterfield, D. M. (2011). A self referencing platinum nanoparticle decorated enzyme-based microbiosensor for real time measurement of physiological glucose transport. *Biosensors and Bioelectronics, 26*(5), 2237-2245. doi:http://dx.doi.org/10.1016/j.bios.2010.09.041

48. Shi, J., McLamore, E. S., Jaroch, D., Claussen, J. C., Mirmira, R. G., Rickus, J. L., & Porterfield, D. M. (2011). Oscillatory glucose flux in INS 1 pancreatic β cells: A self-referencing microbiosensor study. *Analytical Biochemistry, 411*(2), 185-193. doi:http://dx.doi.org/10.1016/j.ab.2010.12.019

49. Claussen, J. C., Wickner, M. M., Fisher, T. S., & Porterfield, D. M. (2011). Transforming the Fabrication and Biofunctionalization of Gold Nanoelectrode Arrays into Versatile Electrochemical Glucose Biosensors. *ACS Applied Materials & Interfaces, 3*(5), 1765-1770. doi:10.1021/am200299h

50. Claussen, J. C., Franklin, A. D., ul Haque, A., Porterfield, D. M., & Fisher, T. S. (2009). Electrochemical Biosensor of Nanocube-Augmented Carbon Nanotube Networks. *ACS Nano, 3*(1), 37-44. doi:10.1021/nn800682m

51. Marr, K. M., Chen, B., Mootz, E. J., Geder, J., Pruessner, M., Melde, B. J., . . . Claussen, J. C. (2015). High Aspect Ratio Carbon Nanotube Membranes Decorated with Pt

Nanoparticle Urchins for Micro Underwater Vehicle Propulsion via H2O2 Decomposition. *ACS Nano, 9*(8), 7791-7803. doi:10.1021/acsnano.5b02124

52. Claussen, J. C., Daniele, M. A., Geder, J., Pruessner, M., Mäkinen, A. J., Melde, B. J., . . . Medintz, I. L. (2014). Platinum-Paper Micromotors: An Urchin-like Nanohybrid Catalyst for Green Monopropellant Bubble-Thrusters. *ACS Applied Materials & Interfaces, 6*(20), 17837-17847. doi:10.1021/am504525e

53. Claussen, J. C., Artiles, M. S., McLamore, E. S., Mohanty, S., Shi, J., Rickus, J. L., . . . Porterfield, D. M. (2011). Electrochemical glutamate biosensing with nanocube and nanosphere augmented single-walled carbon nanotube networks: a comparative study. *Journal of Materials Chemistry, 21*(30), 11224-11231. doi:10.1039/C1JM11561H

54. Claussen, J. C., Kim, S. S., Haque, A., Artiles, M. S., Porterfield, D. M., & Fisher, T. S. (2010). Electrochemical Glucose Biosensor of Platinum Nanospheres Connected by Carbon Nanotubes. *Journal of Diabetes Science and Technology, 4*(2), 312-319. doi:10.1177/193229681000400211

55. Banks, C. E., Davies, T. J., Wildgoose, G. G., & Compton, R. G. (2005). Electrocatalysis at graphite and carbon nanotube modified electrodes: edge-plane sites and tube ends are the reactive sites. *Chemical Communications*(7), 829-841. doi:10.1039/B413177K

56. King, H., Aubert, R. E., & Herman, W. H. (1998). Global Burden of Diabetes, 1995–2025: Prevalence, numerical estimates, and projections. *Diabetes Care, 21*(9), 1414-1431. doi:10.2337/diacare.21.9.1414

57. Ginsberg, B. H. (1992). An overview of minimally invasive technologies. *Clinical Chemistry, 38*(9), 1596-1600. Retrieved from http://www.clinchem.org/content/38/9/1596.abstract

58. Shapiro, Y., Pandolf, K. B., & Goldman, R. F. (1982). Predicting sweat loss response to exercise, environment and clothing. *European Journal of Applied Physiology and Occupational Physiology, 48*(1), 83-96. doi:10.1007/bf00421168

59. Taylor, N. A., & Machado-Moreira, C. A. (2013). Regional variations in transepidermal water loss, eccrine sweat gland density, sweat secretion rates and electrolyte composition in resting and exercising humans. *Extreme Physiology & Medicine, 2*(1), 1-30. doi:10.1186/2046-7648-2-4

60. Huang, S. H., Liu, P., Mokasdar, A., & Hou, L. (2013). Additive manufacturing and its societal impact: a literature review. *The International Journal of Advanced Manufacturing Technology, 67*(5), 1191-1203. doi:10.1007/s00170-012-4558-5

61. Li, J., Rossignol, F., & Macdonald, J. (2015). Inkjet printing for biosensor fabrication: combining chemistry and technology for advanced manufacturing. *Lab on a Chip, 15*(12), 2538-2558. doi:10.1039/C5LC00235D

62. Eggenhuisen, T. M., Galagan, Y., Biezemans, A. F. K. V., Slaats, T. M. W. L., Voorthuijzen, W. P., Kommeren, S., . . . Groen, W. A. (2015). High efficiency, fully inkjet printed organic solar cells with freedom of design. *Journal of Materials Chemistry A, 3*(14), 7255-7262. doi:10.1039/C5TA00540J

63. Azzellino, G., Grimoldi, A., Binda, M., Caironi, M., Natali, D., & Sampietro, M. (2013). Fully Inkjet-Printed Organic Photodetectors with High Quantum Yield. *Advanced Materials, 25*(47), 6829-6833. doi:10.1002/adma.201303473

64. Buanz, A. B. M., Saunders, M. H., Basit, A. W., & Gaisford, S. (2011). Preparation of Personalized-dose Salbutamol Sulphate Oral Films with Thermal Ink-Jet Printing. *Pharmaceutical Research, 28*(10), 2386-2392. doi:10.1007/s11095-011-0450-5

65. Das, S. R., Nian, Q., Cargill, A. A., Hondred, J. A., Ding, S., Saei, M., . . . Claussen, J. C. (2016). 3D Nanostructured Inkjet Printed Graphene via UV-Pulsed laser Irradiation Enables Paper-Based Electronics and Electrochemical Devices. *Nanoscale*. doi:10.1039/C6NR04310K

66. Kordás, K., Mustonen, T., Tóth, G., Jantunen, H., Lajunen, M., Soldano, C., . . . Ajayan, P. M. (2006). Inkjet printing of electrically conductive patterns of carbon nanotubes. *Small, 2*(8-9), 1021-1025.

67. Venkatanarayanan, A., Crowley, K., Lestini, E., Keyes, T. E., Rusling, J. F., & Forster, R. J. (2012). High sensitivity carbon nanotube based electrochemiluminescence sensor array. *Biosensors and Bioelectronics, 31*(1), 233-239.

68. Chen, W.-X., Lee, J. Y., & Liu, Z. (2004). Preparation of Pt and PtRu nanoparticles supported on carbon nanotubes by microwave-assisted heating polyol process. *Materials Letters, 58*(25), 3166-3169. doi:http://dx.doi.org/10.1016/j.matlet.2004.06.008

69. Yu, R., Chen, L., Liu, Q., Lin, J., Tan, K.-L., Ng, S. C., . . . Hor, T. S. A. (1998). Platinum Deposition on Carbon Nanotubes via Chemical Modification. *Chemistry of Materials, 10*(3), 718-722. doi:10.1021/cm970364z

70. Weibel, M. K., & Bright, H. J. (1971). The glucose oxidase mechanism interpretation of the pH dependence. *Journal of Biological Chemistry, 246*(9), 2734-2744.

71. Weng, B., Morrin, A., Shepherd, R., Crowley, K., Killard, A. J., Innis, P. C., & Wallace, G. G. (2014). Wholly printed polypyrrole nanoparticle-based biosensors on flexible substrate. *Journal of Materials Chemistry B, 2*(7), 793-799. doi:10.1039/C3TB21378A

72. Setti, L., Fraleoni-Morgera, A., Ballarin, B., Filippini, A., Frascaro, D., & Piana, C. (2005). An amperometric glucose biosensor prototype fabricated by thermal inkjet printing. *Biosensors and Bioelectronics, 20*(10), 2019-2026. doi:http://dx.doi.org/10.1016/j.bios.2004.09.022

73. Wang, T., Cook, C., & Derby, B. (2009). *Fabrication of a glucose biosensor by piezoelectric inkjet printing.* Paper presented at the Sensor Technologies and Applications, 2009. SENSORCOMM'09. Third International Conference on.

74. Kang, X., Wang, J., Wu, H., Aksay, I. A., Liu, J., & Lin, Y. (2009). Glucose Oxidase–graphene–chitosan modified electrode for direct electrochemistry and glucose sensing. *Biosensors and Bioelectronics, 25*(4), 901-905. doi:http://dx.doi.org/10.1016/j.bios.2009.09.004

75. Jin, S., Jonathan, C. C., Eric, S. M., Aeraj ul, H., David, J., Alfred, R. D., . . . Porterfield, D. M. (2011). A comparative study of enzyme immobilization strategies for multi-walled carbon nanotube glucose biosensors. *Nanotechnology, 22*(35), 355502. Retrieved from http://stacks.iop.org/0957-4484/22/i=35/a=355502

76. Ahmad, R., Vaseem, M., Tripathy, N., & Hahn, Y.-B. (2013). Wide Linear-Range Detecting Nonenzymatic Glucose Biosensor Based on CuO Nanoparticles Inkjet-Printed on Electrodes. *Analytical Chemistry, 85*(21), 10448-10454. doi:10.1021/ac402925r

77. Abe, K., Suzuki, K., & Citterio, D. (2008). Inkjet-Printed Microfluidic Multianalyte Chemical Sensing Paper. *Analytical Chemistry, 80*(18), 6928-6934. doi:10.1021/ac800604v

78. Yun, Y. H., Lee, B. K., Choi, J. S., Kim, S., Yoo, B., Kim, Y. S., . . . Cho, Y. W. (2011). A Glucose Sensor Fabricated by Piezoelectric Inkjet Printing of Conducting Polymers and Bienzymes. *Analytical Sciences, 27*(4), 375-375. doi:10.2116/analsci.27.375

79. Newman, J. D., Turner, A. P. F., & Marrazza, G. (1992). Ink-jet printing for the fabrication of amperometric glucose biosensors. *Analytica Chimica Acta, 262*(1), 13-17. doi:http://dx.doi.org/10.1016/0003-2670(92)80002-O

80. Zhang, Y., Lyu, F., Ge, J., & Liu, Z. (2014). Ink-jet printing an optimal multi-enzyme system. *Chemical Communications, 50*(85), 12919-12922. doi:10.1039/C4CC06158F

APPENDIX

PT-CNT FABRICATION PROCEDURES

Microwave Method: procedure adapted from Chen 2004 (ref. 67) and Yu 1998 (ref. 68)

0.25 mL of an aqueous solution of 0.05 M $H_2PtCl_6 \cdot 6H_2O$ was mixed with 6.25 mL of ethylene glycol and 0.1 mL of 0.4 M KOH in a glass beaker. CNTs (10 mg) were dispersed in the aforementioned solution and dispersed via bath sonication for 30 minutes. After sonication, the solution was microwaved in a beaker at 700 W for 50 seconds. The suspension was then centrifuged at 12000 rpm for 5 min, and the resulting precipitate was rinsed with acetone (centrifuged at 12000 rpm for 5 min, replaced acetone and centrifuged again; process repeated 3 times).

Chemical Method: procedure adapted from Claussen 2014 (ref. 52)

36 mL deionized water (18.2 MΩ-cm) was mixed with 4 ml formic acid in a glass beaker and 58 mg $H_2PtCl_6 \cdot 6H_2O$ followed by 5.3 mg CNTs were added to the solution. The resulting mixture was bath sonicated for thirty minutes. The pH was not adjusted. The mixture was coated in parafilm and allowed to sit at room temperature for the reaction to proceed to completion. After approximately three days the reaction finished, and the mixture was centrifuged. The resulting precipitate was rinsed with acetone and centrifuged three additional times.

Ink Formulation: Pt-CNTs formed by both methods were dispersed via bath sonication for 30 min in DMF at a concentration of 0.3 mg/mL to make the microwave-DMF

ink and the chemical-DMF ink. The microwave-SDS and chemical-SDS inks were created by dispersing (again, via bath sonication for 30 min) 0.3 mg/mL Pt-CNTs in 3 mg/mL SDS in deionized water. The microwave-DMF ink was filtered with a 0.8 μm syringe filter prior to inkjet printing. Ink was stored at room temperature, as low temperature was found to cause irreversible particle sedimentation.